Geophys. J. Int. (2000) **143,** 185–203

A precisely dated Proterozoic palaeomagnetic pole from the North China craton, and its relevance to palaeocontinental reconstruction

Henry C. Halls,[1] Jianghai Li,[2] Don Davis,[3] Guiting Hou,[2] Baoxing Zhang[1] and Xianglin Qian[2]

[1] *Department of Geology, University of Toronto at Mississauga, Mississauga, Ontario, Canada* L5L 1C6. *E-mail: hhalls@credit.erin.utoronto.ca*
[2] *Department of Geology, Peking University, Beijing* 100871, *People's Republic of China*
[3] *Jack Satterly Geochronological Laboratory, Royal Ontario Museum, Toronto, Ontario, Canada,* M5S 2C6

Accepted 2000 May 12. Received 2000 April 25; in original form 1999 November 8

SUMMARY

A palaeomagnetic pole position, derived from a precisely dated primary remanence, with minimal uncertainties due to secular variation and structural correction, has been obtained for China's largest dyke swarm, which trends for about 1000 km in a NNW direction across the North China craton. Positive palaeomagnetic contact tests on two dykes signify that the remanent magnetization is primary and formed during initial cooling of the intrusions. The age of one of these dykes, based on U–Pb dating of primary zircon, is 1769.1 ± 2.5 Ma. The mean palaeomagnetic direction for 19 dykes, after structural correction, is $D = 36^\circ$, $I = -5^\circ$, $k = 63$, $\alpha_{95} = 4^\circ$, yielding a palaeomagnetic pole at Plat = 36°N, Plong = 247°E, $dp = 2^\circ$, $dm = 4^\circ$ and a palaeolatitude of 2.6°S. Comparison of this pole position with others of similar age from the Canadian Shield allows a continental reconstruction that is compatible with a more or less unchanged configuration of Laurentia, Siberia and the North China craton since about 1800 Ma

Key words: China, dykes, palaeomagnetism, Palaeoproterozoic, U–Pb geochronology.

1 INTRODUCTION

A key palaeomagnetic pole (Buchan *et al.* 1994; 2000) is one that is reliable both in position and age and serves as an anchor point through which an apparent polar wander path (apwp) for a continent must be drawn. The precise definition of apwps is essential before continental reconstructions can be accepted, especially those in the Precambrian (e.g. Moores 1991; Hoffman 1991), where juxtaposed cratons may have had completely different configurations from Phanerozoic Pangaea. In this paper we present palaeomagnetic and U–Pb age data for a major Palaeoproterozoic dyke swarm from the North China craton (NCC) in an attempt to establish a key pole from a craton for which the apwp is largely derived from sedimentary units (Zhang 1998).

A palaeomagnetic pole becomes a key pole when (1) the nature of the remanence, whether primary or secondary, is demonstrated through adequate field tests; (2) any structural correction is known; (3) secular variation is averaged out; and (4) the age of the remanence is precisely dated using radiometric methods on the same rocks as those from which the remanence has been obtained. The acquisition of key poles from the earlier part of Precambrian times is a particular challenge because sampled units are often altered and deformed to varying degrees by later geological events.

In the NCC, a NNW-trending dyke swarm known as the Taihang dyke swarm (Li 1999) (Fig. 1) was selected for study because (1) previous reconnaissance palaeomagnetic work had indicated stable remanences (Qian & Chen 1987; Zhang 1988), and (2) the dyke swarm is unmetamorphosed, and may represent the first igneous event to occur after reworking of the shield in the Palaeoproterozoic.

2 GENERAL GEOLOGY OF THE NORTH CHINA CRATON

Basement rocks of the north-central part of the NCC, which comprise aluminous metasediments (khondalites), grey tonalitic gneisses, and greenstones with interlayered clastics, were intruded by granites and cratonized between 2.4 and 2.6 Ga (Li *et al.* 1997). They form a series of relatively mountainous inliers in faulted contact with younger Proterozoic, Palaeozoic and Mesozoic strata that underlie intervening valleys (Fig. 1). Along the northern margin of the NCC is a major (2.5–1.8 Ga) Palaeoproterozoic orogen which may have also reworked much of the NCC, as shown by U–Pb dates of 1.8–2.0 Ga on granulite to amphibolite-facies basement gneisses (Zhai *et al.* 1996; Li *et al.* 1997; Guo & Shi 1996), and by the presence in the NCC of potassic granites with U–Pb zircon ages of 2.1 Ga (e.g. Wilde *et al.* 1997; Guo & Shi 1996). The regional metamorphic

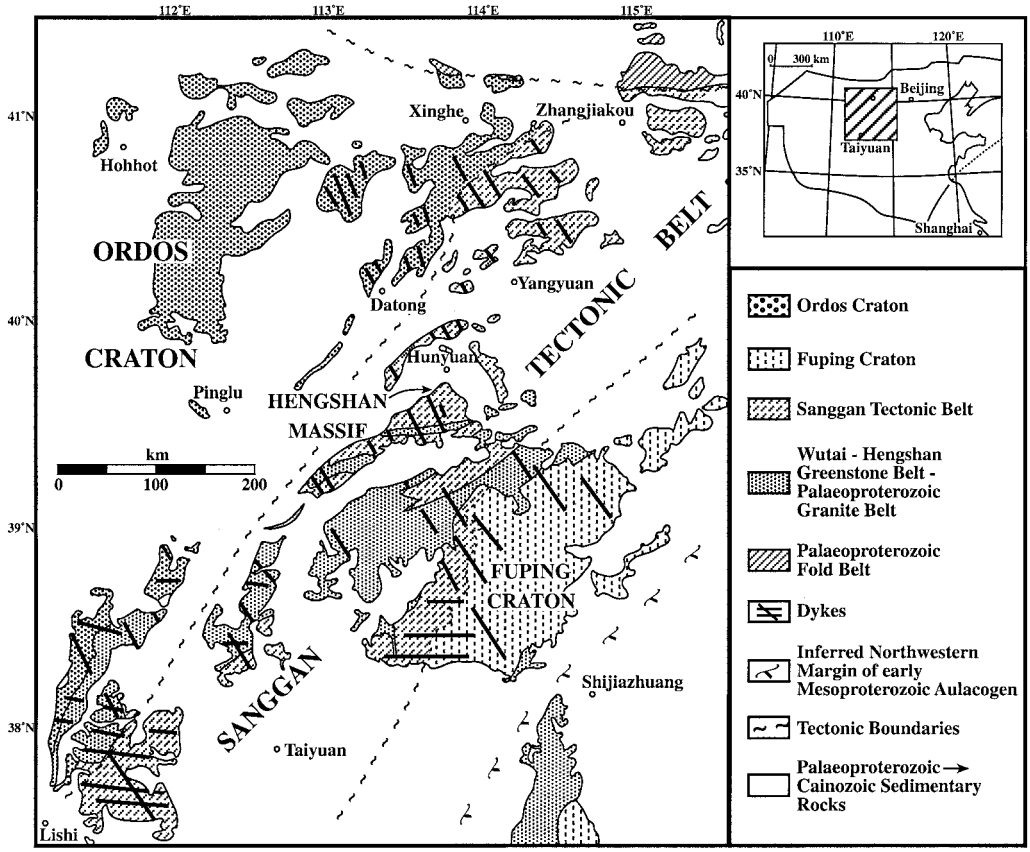

Figure 1. General geological map of the NCC. Inset map shows the extent of NCC and the location of the study area.

grade of the NCC generally decreases to the S and SW, from granulite facies approximately north of Datong (Fig. 1) to amphibolite facies in the Hengshan Massif and Fuping craton (Li *et al.* 1997).

Southeast of the Fuping Craton (Fig. 1) is a NE-trending fault-bounded trough of sedimentary and volcanic rocks (the 1.4–1.0 Ga Jixian and 1.4–1.8 Ga Changcheng systems). Volcanics in the lower part of the Changcheng sequence crop out at the extreme northern and southern ends of the trough (Zhao *et al.* 1994). They may exist in the trough SE of the Fuping craton, but younger sedimentary units overlap the lower Changcheng sequence northwards onto the craton. The volcanics have U–Pb ages on zircon ranging from about 1.63 to 1.84 Ga (Li *et al.* 1995; Sun *et al.* 1991). After the Palaeoproterozoic, much of the NCC was covered by late Mesoproterozoic and Palaeozoic sedimentary rocks followed by intense tectonic reworking during the Mesozoic–Cenozoic, especially in its central and eastern parts. A series of NE-trending extensional basins developed between normal faults that define the boundaries of the various Archaean inliers and which led to their uplift and possible rotation. Small Mesozoic granites also occur (Fig. 2), and, in the Fengzhen inlier, Eocene volcanics locally cap hilltops.

3 PROTEROZOIC DYKE SWARMS

At least two fresh and undeformed dyke swarms, trending NNW and WNW (Fig. 1), cross the North China craton (Qian & Chen 1987; Chen & Shi 1994). The NNW-trending Taihang swarm comprises Fe-rich tholeiites and is cross-cut by more quartz-rich tholeiites of the WNW swarm (Zhang 1988; Hou & Mu 1994). Neither swarm is observed to cut ~1 Ga Neoproterozoic strata, and where these cover rocks are absent, lower Cambrian strata lie unconformably on the dykes (Qian & Chen 1987). Since the dykes are fresh and unmetamorposed, they are younger than about 1.8 Ga, which dates the final stages of the Palaeoproterozoic regional metamorphism. K–Ar whole-rock dating of both dyke sets yields a spectrum of ages between 1.8 and 1.0 Ga, with a concentration in the range 1.6–1.2 Ga (Hou & Mu 1994). These results broadly agree with geological field relations, but also suggest that the two dyke swarms have similar ages. The NNW-trending dykes are observed to cut the Changcheng sequence (Qian & Chen 1987), and therefore the 1.8–1.6 Ga volcanics, found at comparable stratigraphic levels, could represent the same magmatic event.

Palaeomagnetic data from both the WNW- and NNW-trending dykes in the NCC were obtained by Zhang (1988), after initial work by Qian & Chen (1987). The resulting palaeomagnetic directions from both dyke sets plot at shallow inclinations in the NE quadrant of the stereonet, supporting the K–Ar evidence that the ages of the swarms are similar. Zhang's site locations for NNW-trending dykes are shown as BX1 to 5 and BX15 in Fig. 2. Results from these sites will be included with our new data below. A palaeomagnetic study of the granulite host rocks NE of Datong (Zhang & Piper 1994) yielded a swath of directions after thermal demagnetization, generally with shallow positive and negative inclinations, extending through a range of declinations from about 190°, clockwise through N to 060°. Four directional groups were identified

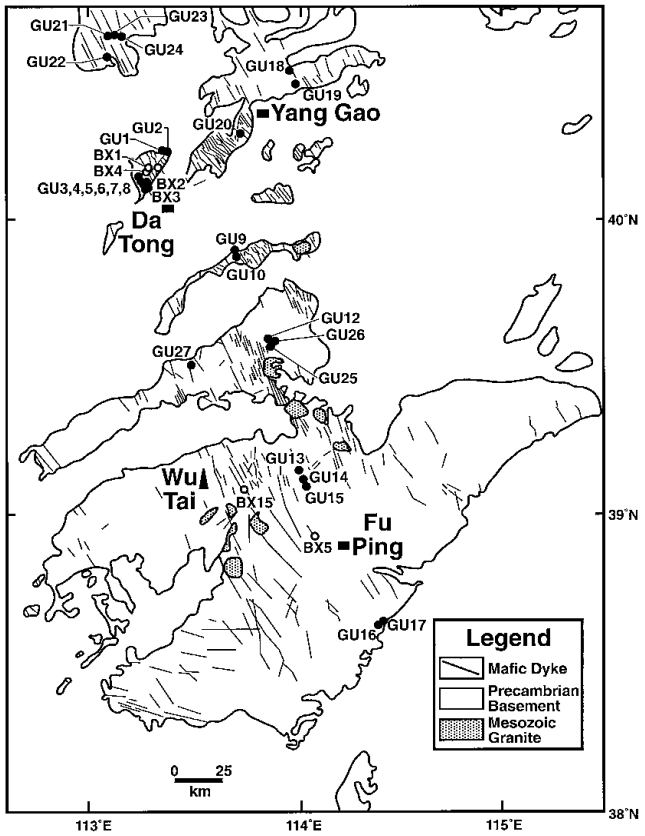

Figure 2. Map showing the location of sampling sites in NNW-trending dykes. The solid dots are from fieldwork carried out in 1996 and 1998, and the open dots are from Zhang (1988). In the text the various cratonic blocks and inliers are informally referred to by the names under which the various sites are grouped in Table 2.

which, after reversing antipodal directions, were found to be $D/I = 57°/-12°$; $28°/-20°$; $5°/-3°$ and $324°/5°$. The relative ages of these components could not be established.

4 FIELD AND EXPERIMENTAL PROCEDURES

4.1 Palaeomagnetism

Oriented samples were obtained from 27 dykes (sites GU1–27) using both a magnetic and sun compass (Fig. 2). The majority of samples were taken from road or river cuts, but seven sites (GU12, 21–26) were in quarries where Taihang dykes are being commercially exploited as decorative and monumental stone. In a few cases (e.g. sites GU6, 7) samples were taken from the fresh centres of spheroidally weathered material, but, from all other sites, fresh samples were taken 5–10 m below the surface weathered zone. Potentially lightning-struck rocks, as determined from *in situ* comparison of magnetic and sun orientations, were avoided. All dykes were NNW-trending except site GU5, which was taken from a younger NE-trending dyke, observed to cross-cut the dyke at site GU4. Samples were either field-drilled or taken as blocks along chilled margins and other places where drilling was not possible. Typically five to six samples were taken per site, but between 10 and 20 were taken for baked contact tests (for example at sites GU12, 19 and 26). Block samples were later cored in the laboratory. All cores were then subject to detailed alternating field (AF) and thermal demagnetization using Schonstedt SD-1 and TSD-1 demagnetizers. In some cases thermal demagnetization was performed on samples previously AF demagnetized. Remanent magnetization was measured on a modified DIGICO magnetometer, for which consistent and repeatable data could be obtained down to magnetization intensities of about 10^{-3} A m^{-1}. Results were analysed using principal component analysis (Kirschvink 1980) with a modified search routine for finding linear segments (Halls 1986).

4.2 Geochronology

Palaeomagnetic core fragments from GU12, weighing about 100 g, were crushed with a jaw crusher and disk mill. About 50 zircon grains were separated using heavy liquids and a Frantz magnetic separator, mostly as highly cracked, colourless fragments. Several relatively fresh fragments were picked and abraded (Krogh 1982). The least cracked, abraded grains were individually spiked with a 205Pb−235U mixture and dissolved in Teflon bombs using HF (Krogh 1973). The samples were dried, re-dissolved in HCl, then dried again and deposited on mass spectrometer filaments with Si-gel and phosphoric acid. A VG354 mass spectrometer equipped with a Daly detector in analogue mode was used for the isotopic analyses. Despite the fact that Zr was not separated from the samples, ion emission was strong and stable on the mass spectrometer over a period of 2–3 hr.

5 SAMPLE PETROGRAPHY

A summary of the main petrographic characteristics of the dykes is given in Fig. 3. It shows that the majority of dykes are composed primarily of plagioclase and clinopyroxene, showing either a subophitic or intergranular texture. The primary texture is visible in all the dykes and well-defined chilled margins are preserved. Olivine may also be present but never exceeds 5 per cent modally. A green amphibole may either rim or replace pyroxene. Myrmekitic intergrowths of quartz and feldspar, often spatially associated with apatite needles, occur when olivine is absent. Biotite and magnetite are also important accessory phases. In general the degree of hydrous alteration involving saussuritization of feldspar, conversion of pyroxene to amphibole, and serpentinization of olivine increases towards the south. At the same time, feldspar clouding, a brown discolouration of the feldspar caused in part by submicroscopic magnetite, which tends to be more intense for more deeply exhumed dykes (e.g. Halls & Zhang 1998), increases towards the north. Therefore dykes in the higher-grade, granulite terranes of the Fengshen, Datong, Tienzhen and Yanggao inliers (Fig. 2) tend to be the least altered, with fresh olivine and feldspars with the highest clouding intensities (Fig. 3). Feldspars exhibiting the lowest clouding and highest alteration levels are found in the Fuping craton (Fig. 3), where chlorite veining and alteration in the dykes are more conspicuous. The feldspar data suggest that the NCC has been tilted a few degrees or less towards the south after the dykes were emplaced (*cf.* Halls & Zhang 1998).

Pleochroic haloes around small grains, mostly zircon, are common in GU12 and 27, less abundant at sites GU8, 16, 18–20, 22 and 26, and rare or absent in the remaining dykes. The haloes are typically found in primary amphibole and less often in biotite.

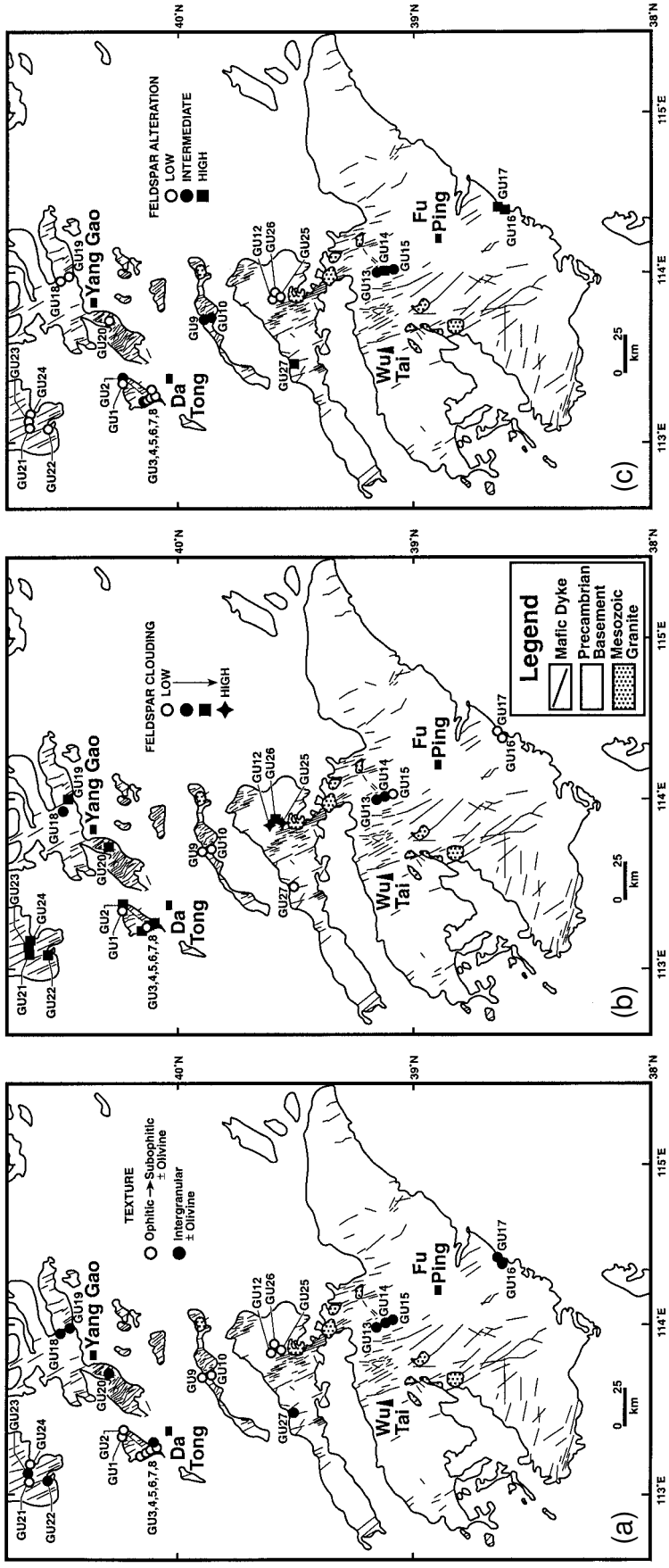

Figure 3. Maps summarizing variations in three petrographic features of the Taihang dyke swarm at the sampled localities: (a) texture, (b) feldspar clouding intensity, and (c) feldspar alteration.

6 U–PB GEOCHRONOLOGY RESULTS

Analytical results for dyke GU12 are presented in Table 1 (errors given at 1 sigma) and plotted in Fig. 4 (error ellipses plotted at 2 sigma). Regressions were carried out using the program of Davis (1982). Age errors are quoted at 95 per cent confidence. Four of the present analyses show Th/U ratios above the value ($\sim$0.3–0.8) expected for zircon in quartz-bearing felsic rocks (Ahrens *et al.* 1967). Such relatively high Th/U ratios are often found for zircons crystallized from mafic magmas (Heaman *et al.* 1990), and argue that these zircons are not xenocrystic. A fifth analysis shows an exceptionally low Th/U ratio. This grain was assumed to be a zircon fragment during picking and was the only brown grain analysed. Because of its low Th/U ratio and colour, it is considered likely that the grain was baddeleyite, an occasional trace mineral in mafic igneous rocks (Heaman & LeCheminant 1993). The baddeleyite and one zircon data point are nearly concordant. Regressing all five data points gives an upper intercept age of 1769.1 $\pm$ 2.5 Ma with a 26 per cent probability of fit. The fit probability is

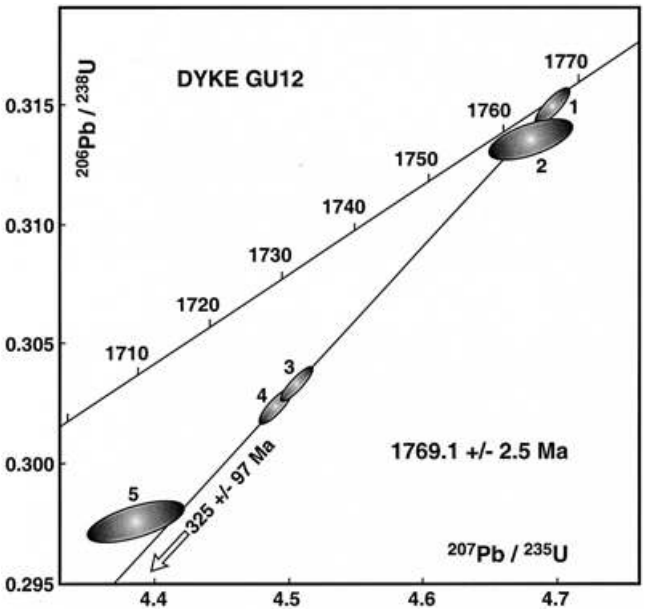

Figure 4. Concordia diagram showing U–Pb data points from analyses of zircon (1, 3, 4 and 5) and probable baddeleyite (2) in dyke GU12. The regression line to all the data points is also shown.

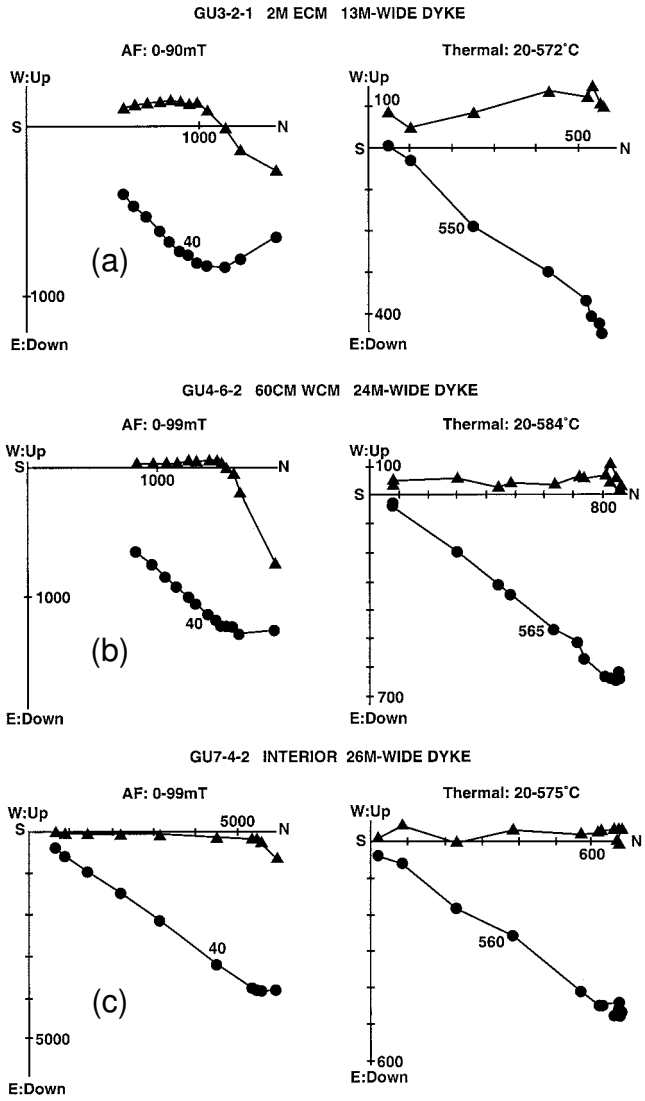

Figure 5. Diagrams (a), (b) and (c) are vector diagrams after AF followed by thermal demagnetization, for samples from three dyke sites (GU3, 4, and 7). Note the high-coercivity and high-unblocking-temperature component A and its directional stability down to intensities of less than 10 per cent of initial value, and the PEF-like low-coercivity component. On vector diagrams in this and all remaining figures, dots/triangles are projections on the horizontal/vertical plane, respectively, and magnetization intensity units are A $m^{-1} \times 10^{-3}$.

Table 1. Analytical results of single zircon U–Pb mass spectrometry.

No.	Fraction	Weight (mg)	U (ppm)	Th/U	PbCom Pg	207/204	206/238	1 sigma	207/235	1 sigma	207/206 Age (Ma)	1 sigma	% Disc.
	Mafic Dyke GU12												
1	1 Ab zr, pink	0.0002	1425	1.03	0.7	892.6	0.31494	0.00035	4.6959	0.0063	1768.3	1.1	0.2
2	1 Ab bad, brn, cracked	0.0005	256	0.09	0.5	565.3	0.31360	0.00040	4.6793	0.0150	1769.6	4.7	0.7
3	1 Ab zr, clr, cracked	0.0010	773	3.07	0.4	4712.8	0.30326	0.00032	4.5060	0.0057	1762.0	0.9	3.5
4	1 Ab zr, flat, clr	0.0003	1125	0.68	1.1	681.2	0.30236	0.00032	4.4897	0.0060	1760.8	1.2	3.7
5	1 Ab zr, elong frag, clr	0.0003	1906	1.84	13.8	99.9	0.29757	0.00041	4.3855	0.0175	1747.0	6.0	4.4

Errors are given at 1 sigma.
Ab: abraded; zr: zircon grain; elong: elongate; frag: fragment, clr: colourless; brn: brownish.
PbCom: Common Pb, assuming all has blank isotopic composition.
Th/U calculated from radiogenic 208Pb/206Pb ratio and 207Pb/206Pb age assuming concordance.
% Disc: per cent discordance for the given 207Pb/206Pb age.

Table 2. Summary of palaeomagnetic results for NNW-trending dykes from the North China craton.

Site	CRP	Trend[°]	Dip[°]	Width[M]	NS	T	D[°]	I[°]	k	α_{95}[°]
FENGZHEN INLIER										
GU21	Q	340	90	31	10	AF	46.7	−15.4*	92	5.1
GU22	Q	310	90	40	7	AF,TH	38.3	−7.1*	225	4.0
GU23	Q	340	40E	10	8	AF,TH	37.4	−6.0*	79	6.3
GU24	Q	338	90	20	9	AF,TH	44.3	−0.4*	122	4.7
MEAN					4	AF,TH	41.6	−7.2	113	8.7
TIANZHEN INLIER										
GU18	N	336	90	>25	7	AF,TH	28.5	5.4*	844	2.0
GU19	C	331	90	>19, <40	7	AF,TH	45.5	−13.2*	299	3.5
YANGGAO INLIER										
GU20	C	325	55E	34	9	AF,TH	38.8	−34.2	255	3.2
After structural rotation							42.0	0.0*		
DATONG INLIER										
GU1	N	340	–	>20	5	AF	34.6	−2.4*	1075	2.3
GU2	C	020	–	>25, <40	6	AF	38.1	−6.6	508	3.0
					4	AF,TH	37.5	−9.7*	170	7.1
GU3	C	340	–	13	3	AF	34.5	−5.9	67	15.2
GU4	C	335	90	24	5	AF	32.9	−3.9*	102	7.6
GU6+7	C	335	90	26	8	AF,TH	36.6	−2.0*	571	2.3
GU8	C	340	90	66	5	AF	33.1	−5.5*	340	4.2
BX1	C	335	90	25	5	TH	37.5	3.1*	201	5.4
BX2	C	320	85E	25	5	TH	41.1	4.9*	122	7.0
BX3	C	319	80E	30	4	TH	39.2	−2.6*	264	5.7
BX4	C	330	80E	30	6	TH	37.0	−6.3*	160	5.3
MEAN					9	AF,TH	36.6	−2.7	237	3.4
HUNYUAN INLIER										
GU9	N	315	90	42	5	AF	10.3	−15.9*	92	8.0
GU10	N	320	70W	30	8	AF		NO STABLE END POINTS		
HENGSHAN INLIER										
GU12	Q	320	70E	>65, <100	8	AF	22.8	−26.3	294	3.2
					6	AF+TH	22.7	−29.6	341	3.6
					9	AF,TH	22.7	−28.2	327	2.9
After structural rotation							26.0	−9.0*		
GU12	BAKED TONALITE				2	AF	27.4	−26.0	57	33.8
					4	AF,TH	24.7	−23.9	115	8.6
GU12	UNBAKED TONALITE				2	AF	00.1	−6.5	105	24.6
GU26	Q	336	72E	33	7	AF,TH	31.0	−24.8	81	6.7
After structural rotation							34.5	−11.0*		
GU26	BAKED TONALITE				2	AF,TH	20.8	−27.5	225	16.7
GU26	UNBAKED TONALITE				2	AF	9.3	−2.4	31	46.0
WUTAI-FUPING CRATON										
BX5	C	325	80E	35	3	TH	29.7	−6.4	21	27.6
BX15	C	300	75E	30	3	TH	32.3	−0.2	36	20.9
MISCELLANEOUS SITES										
GU5	N	030	–	54	4	AF	88.9	38.9	216	6.3
GU13	C	335	60W	20	9	AF	34.5	30.7	30	9.5
BAKED HOST ROCKS					7	AF	15.8	27.9	33	10.7
GU14	C	325	50E	58	5	AF	122.0	74.4	67	9.4
GU15	C	340	75E	6	3	AF	24.1	30.5	172	9.4
GU16	Q	310	70E	90	6	AF	140.7	−4.0	8	26.0
GU17	N	320	75E	55	7	AF	12.1	19.5	67	7.0
GU27	Q/C	326	80W	73	11	AF	346.0	52.7	64	5.7
SITE MEAN DIRECTIONS [USING SITES (*) WITH $\alpha_{95} < 10°$]										
With structural rotation (SC):					19	AF,TH	36.0	−5.2	63	4.2
No structural rotation:					19	AF,TH	35.5	−8.7	35	5.7
No SC but including sites GU13,15 & 17:					22	AF,TH	34.0	−3.9	19	7.3

PALAEOMAGNETIC POLES

Lat[°N]	Long[°E]	Plat[°N]	Plong[°E]	dp[°]	dm[°]	Palaeolat[°S]
After structural correction						
40.2	113.5	36.0	247.0	2.1	4.2	2.6
No structural correction						
40.2	113.5	34.8	248.7	2.9	5.7	4.4
No structural correction and includng sites GU13, 15 & 17						
40.2	113.5	37.7	248.6	3.7	7.3	1.9

Symbols: CRP refers to the type of outcrop, whether natural, typically from river valleys (N), a quarry (Q) or a roadcut (C); NS is the number of independently orientated samples; T is the demagnetization treatment: AF—alternating field demagnetization, TH—thermal demagnetization; AF+TH—alternating field followed by thermal demagnetization; AF,TH—included samples may have all three kinds of demagnetization treatment. D, I are declination, inclination of remanence; k is precision parameter, α_{95} is the 95 per cent confidence oval about the mean direction; dp, dm are the lengths of the semi-minor and semi-major axes of the 95 per cent confidence oval about the pole position, which has been calculated using an average site location of Lat. 40.2°N, Long. 113.5°E. On the Van der Voo (1988) quality index Q scale, the Taihang swarm pole rates a score of 5 out of a maximum 7 points, as it lacks antipodal reversals and its position is possibly similar to at least one pole of younger times (the Silurian-Devonian one of Zhao *et al.* 1993). The positive baked contact tests on the local scale are weakened by the presence of the A component in granulites remote from the dykes. If further work shows the field tests to be negative, and therefore the assigned age to be inappropriate, the Q-value could be reduced to 4.

lowered by the most discordant data point, which is also relatively imprecise. The fact that both the near-concordant baddeleyite and high Th/U zircon data agree in age argues strongly that this is the age of emplacement of the dyke. The age of the Taihang dyke swarm, once thought to be about 1250 Ma by Qian & Chen (1987), must now be revised in light of the new U–Pb data.

7 PALAEOMAGNETIC RESULTS

7.1 General characteristics of remanent magnetization

Most dykes, particularly those in the northern inliers, and excluding the Fuping craton, give a well-defined high-coercivity, high-unblocking-temperature remanence A, with shallow negative inclination and NE declination. The only other coherent remanence component (B), with lower coercivity and unblocking temperature, has a direction compatible with the present Earth's field direction (D/I = 357°/58°), but could also reflect mild reheating during Mesozoic or Cenozoic magmatism. Thermal demagnetization data (Fig. 5) suggest that the main carrier is magnetite. AF and thermal demagnetization data gave comparable results for different specimen cores of the same sample, although in a few cases the thermal stable endpoint had a negative inclination up to about 5° steeper than that obtained by AF demagnetization. This result was confirmed when specimen cores were subjected to AF followed by thermal demagnetization (Fig. 5).

A summary of the palaeomagnetic results, subdivided according to inlier, is given in Table 2. A group of miscellaneous dykes, mostly at the southern end of the swarm in the Fuping craton, where alteration levels are higher, generally did not give A. The NE-trending dyke at site GU5 and also the NW-trending dyes at sites GU14 and 27 may represent different ages of intrusion from the Taihang swarm. Sites GU13 and 15 both included samples that moved towards A at higher demagnetization fields, and therefore are likely to be Taihang dykes. These dykes, and also GU16 and 17, appear to be overprinted. Two remaining sites (GU11 and 25) were not analysed, the former due to severe weathering and the latter because drilling was suspended when it was discovered that site GU12, about 1 km away, had sampled the same dyke.

In the following section we consider the age of A in terms of whether it represents a primary component, in which case it is 1770 Ma, or a secondary one with a significantly younger age—a distinct possibility because a pre-folding primary remanence with a direction very similar to A has been obtained from Silurian and Devonian strata along the western margin of the North China craton (Zhao *et al.* 1993). We approach this problem with a discussion of three baked contact tests that were carried out at sites GU12, 19 and 26. In all three cases the host rocks were fine-grained grey tonalitic gneisses in upper amphibolite to granulite grades of regional metamorphism, which, from previous experience with similar rocks from the Kapuskasing zone in Canada (e.g. Halls *et al.* 1994), are frequent carriers of stable remanence.

7.2 Baked contact tests

7.2.1 Site GU12

This site, which is of critical importance since it has been U–Pb dated, is a quarry at the top of a mountain (Fig. 6). Both AF and thermal demagnetization of dyke interior and chilled margin samples (Fig. 7) give the same characteristic direction as baked host rock samples (Fig. 8). Two host rock samples collected at distances greater or equal to one dyke width gave a significantly different direction of $D \sim 000°$, $I = -7°$ (Fig. 9). This magnetization does not occur in the dyke (Fig. 10) and

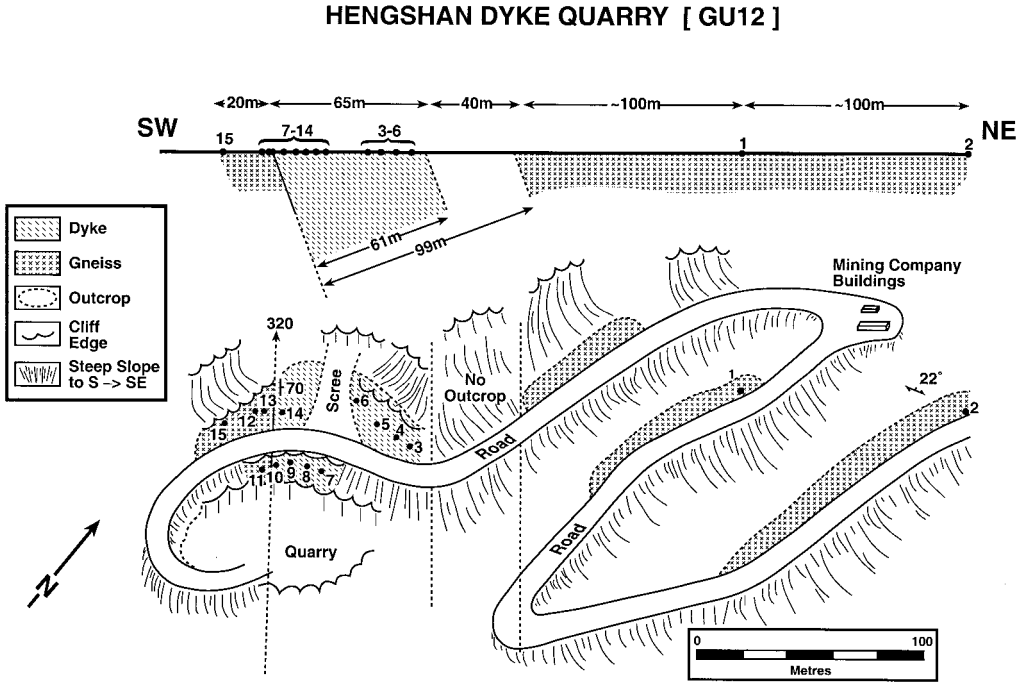

Figure 6. Detailed map of the Hengshan dyke site GU12, showing numbered drilling localities.

therefore it is considered to predate intrusion. The results from site GU12 thus constitute a positive baked contact test, indicating that the remanence in the dyke was acquired during initial cooling.

7.2.2 *Site GU26*

This site, about 1 km to the east of GU12, also occurs in an east-dipping dyke, where samples have been taken from both a

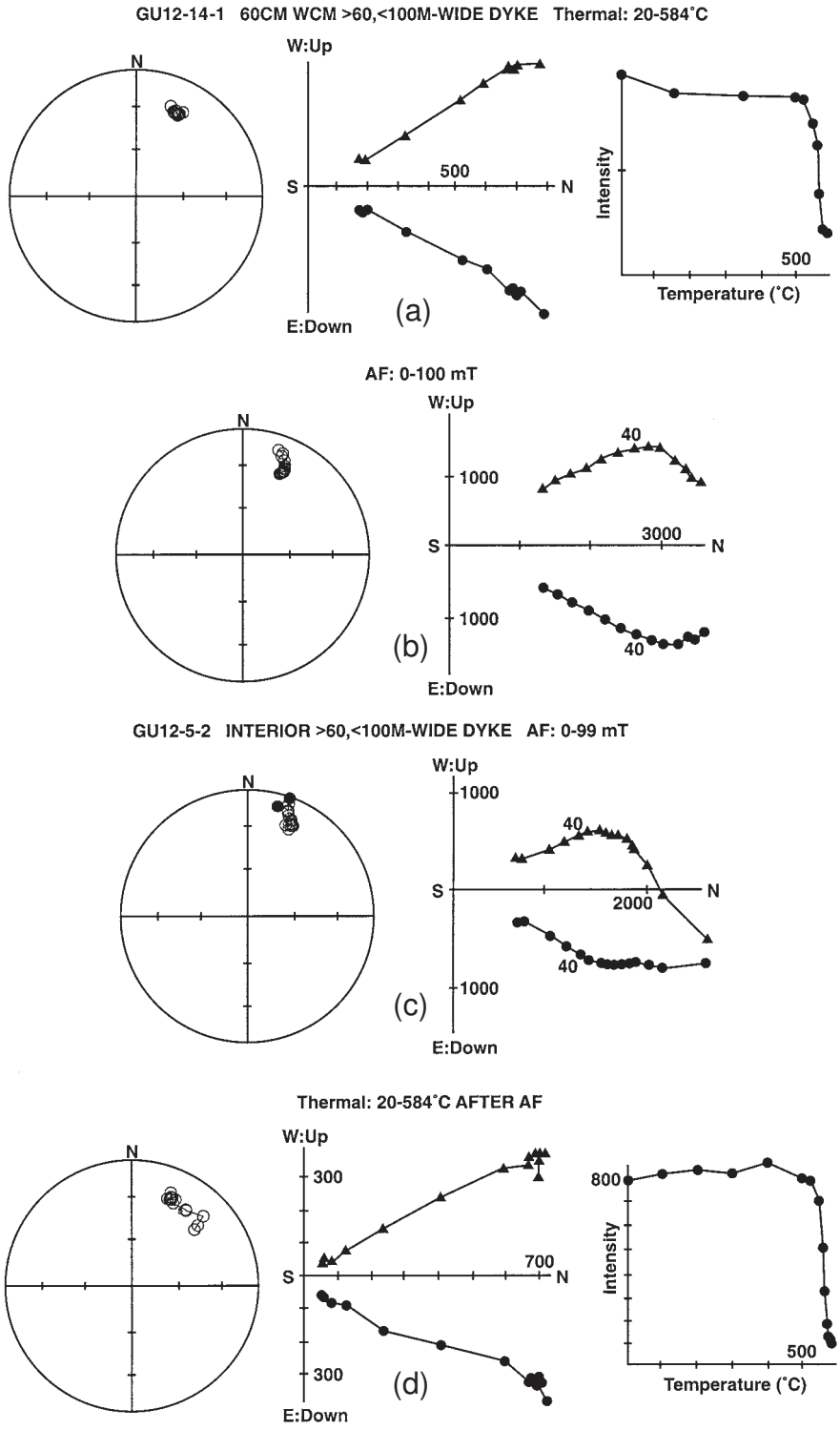

Figure 7. (a) and (d): equal-area stereonets, vector diagrams and intensity decay plots after thermal demagnetization, of samples GU12-14-1 and GU12-5-2, previously AF demagnetized (diagrams b and c, respectively). Note that the AF and thermal treatments reveal the same magnetization component A with a high coercivity/unblocking temperature, and that the fine-grained dyke margin, which is often susceptible to alteration, gives the same results as the dyke interior. Symbols on vector diagrams as in Fig. 5. On stereonets, as in all subsequent figures, open/closed dots are plotted on upper/lower hemispheres. In Figs 7 to 10, sample locations are referenced to eastern or western chilled margins (ECM, WCM) for a dyke with a width of between 60 and 100 m.

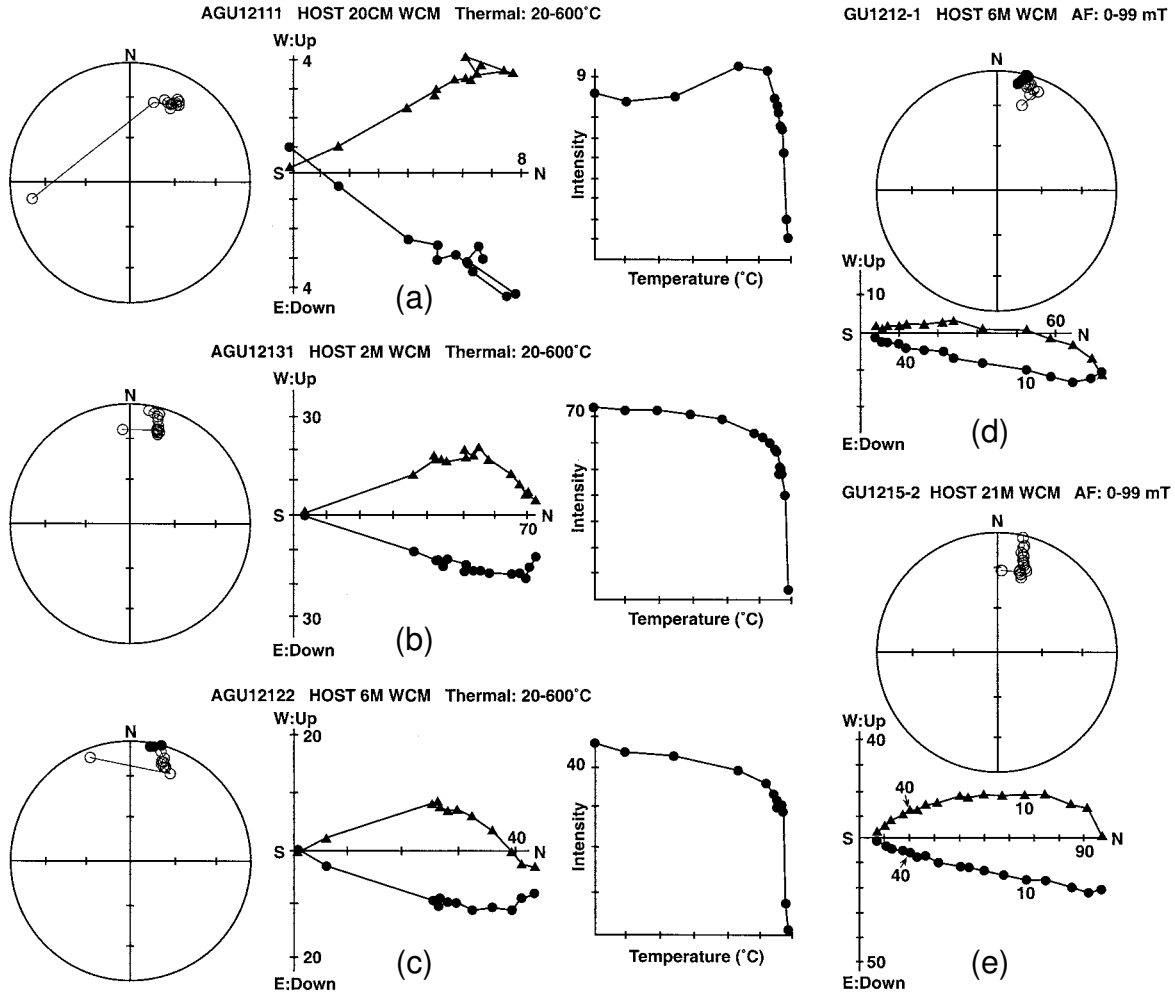

Figure 8. (a) to (c): equal-area stereonets, vector diagrams and intensity decay plots after thermal demagnetization of host rock gneisses from three locations within the baking zone of dyke GU12. (d) and (e) are two samples after AF demagnetization only. (c) and (d) are from companion specimens of the same sample to illustrate the similarity in directional response regardless of the type of demagnetization treatment. Note that all samples yield the A magnetization in the higher coercivity/unblocking-temperature ranges.

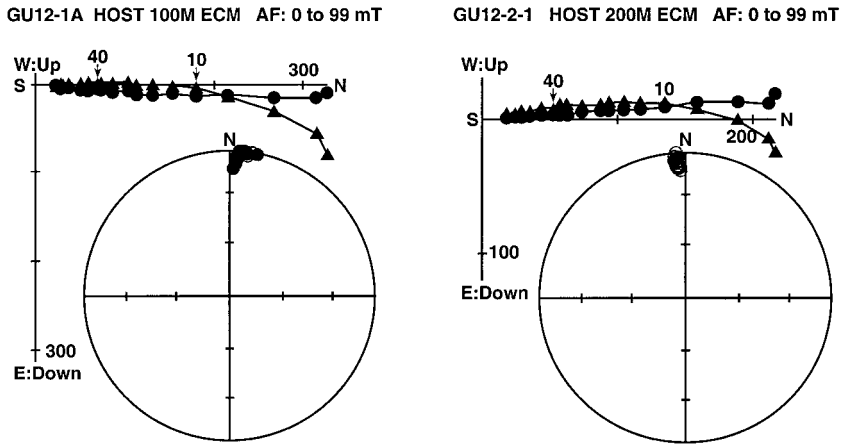

Figure 9. Stereoplot–vector diagram pairs, after AF demagnetization, for samples GU12-1 and GU12-2 in unbaked host rock gneisses, showing a high-coercivity magnetization with low inclination and northerly declination. Note that the more easily removed component in the baked rocks (Figs 8b to e) has in contrast a low coercivity/unblocking temperature, a NW declination and steeper inclination.

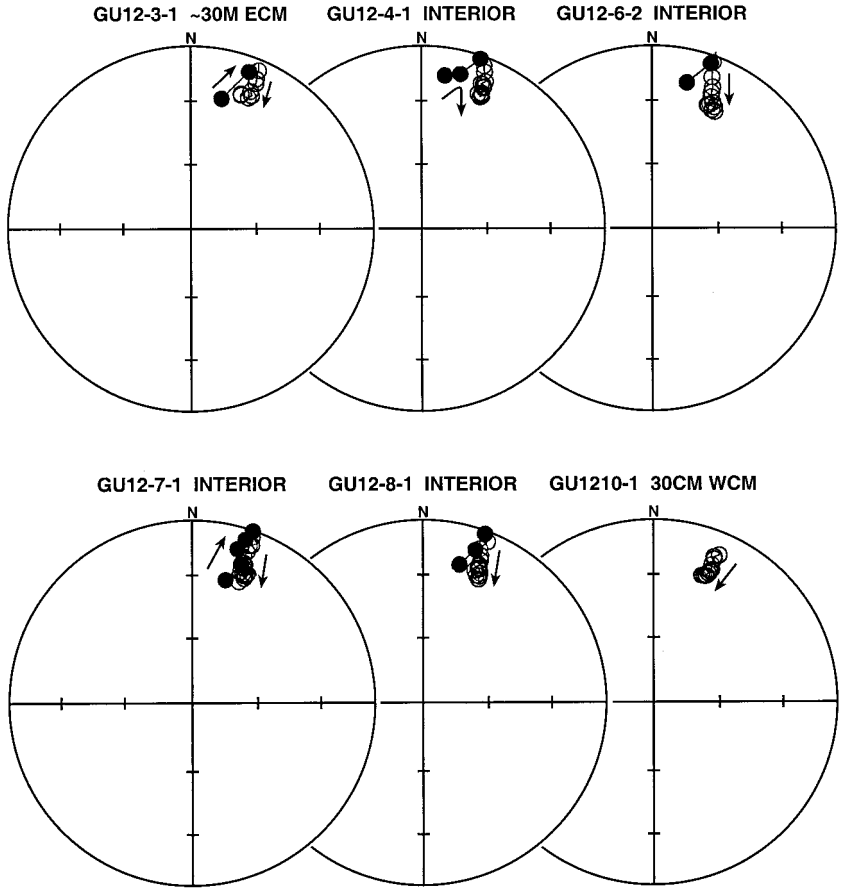

Figure 10. Equal-area stereonets after AF demagnetization from 0 to 100 mT for six dyke samples from site GU12. Note that the great-circle demagnetization trajectories in all cases are consistent with removal of a PEF-like component and show no sign of the flat-lying northerly directed component seen in the unbaked host rocks.

road cut and a quarry (Fig. 11). The results (Fig. 12) are virtually identical to those for site GU12. Despite the proximity of sites GU12 and 26 to a Mesozoic granite intrusion about 5 km distant (Fig. 2), there appears to be no sign of overprinting, unless it is represented by the B component.

7.2.3 Site GU19

This site is taken along a roadcut, where the full width of the dyke is unknown because the eastern margin of the dyke is not exposed (Fig. 13). The results (Fig. 14) show that the dyke (Figs 14a and b) and clearly baked host rocks (Figs 14c to e) have the same characteristic A direction. The most distant host rock sample has a significantly different direction (Fig. 14f), which resembles that in the unbaked host rocks of sites GU12 and 26. Despite the similarity of the data to sites GU12 and 26, the contact test is inconclusive because of the unknown dyke width. Taken as a whole, however, the foregoing results provide convincing evidence that the A magnetization was acquired during initial cooling of the dykes.

7.3 Structural correction of palaeomagnetic data

If the A directions for all sites are plotted without any structural correction, they group closely (Fig. 15a), but three sites (GU12, 20 and 26) have noticeably steeper inclinations. With reference to Table 2, dykes of the Taihang swarm are either vertical, especially towards the north, or have a general easterly dip. Of all the A dykes, sites GU12, 20 and 26 have the shallowest dips, although some sites, notably BX5 and 15, have comparable dips but give the typical shallow A inclination. The three anomalous sites occur in regions more than 40 km from vertical dykes with the shallow A component, and also more or less in separate inliers. We therefore have the freedom to restore dykes GU12, 26 and 20 to the vertical by rotating them about their strike (a minimum rotation), and in doing so to move their anomalous A directions into the main cluster, as shown in Fig. 15(b). A summary of host rock foliation measurements at each site shows that foliation strikes are either to the NE or NW. Although more data are obviously needed, the regionally anomalous foliation strikes observed at the three sites become more consistent with those at other sites after structural correction (Fig. 16). In the vicinity of GU12, fold hinges of the gneissic foliation plunge about 40°SW, in contrast to a more regional average plunge of about 10°–20° to the SW and W across the NCC (Li & Qian 1994, their Fig. 7-2). This observation together with a general southwesterly decrease in metamorphic grade of the host rocks, and a change from tonalitic gneiss to supracrustals (Yan *et al.* 1996), suggests that the Hengshan inlier has been tilted up to the NE, probably in Phanerozoic times. In support of this interpretation, sites

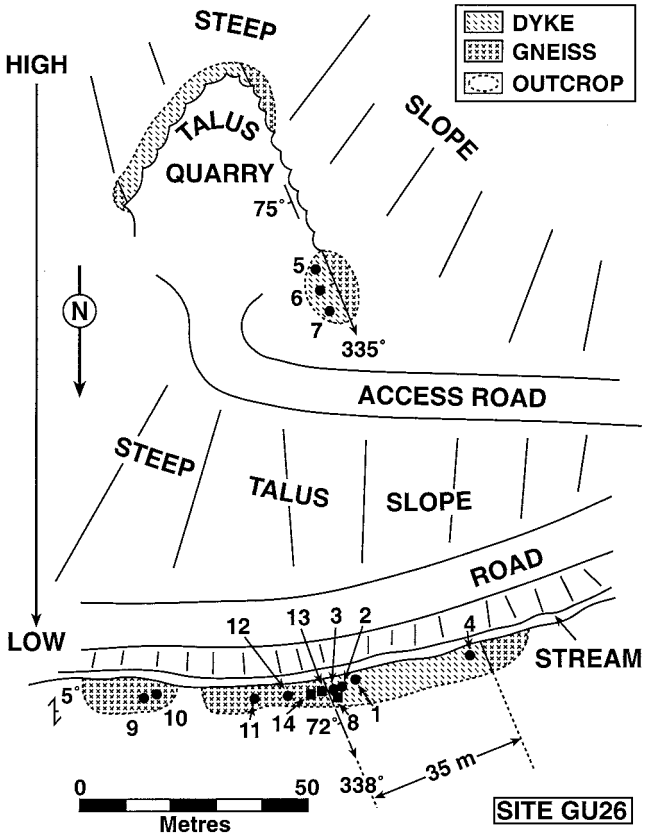

Figure 11. Detailed map of dyke site GU26, showing numbered sampling localities. Round/square points are drilled cores/block samples.

GU12 and 26 possess the deepest levels of feldspar clouding, suggesting a greater post-dyke uplift than elsewhere along the swarm. However, the W to SW tilt cannot be confirmed by other observations; the 70 m wide dyke at site GU27 dips 80° to the *west*, and Proterozoic rocks resting on the basement a few kilometres away dip about 5°NE.

An alternative structural analysis is to assume that no rotation has taken place, in view of the general easterly dip of the swarm as a whole, especially in the Fuping inlier. In this inlier, however, the dykes are more altered and do not give clear A directions (Table 2). Many of the dykes here (GU14, 16, and 17) are extremely thick and coarse-grained and difficult to compare petrologically with the dykes farther north. However, if sites GU12, 26 and 20 have not been rotated, the dispersion of A is increased and therefore sites GU13, 15 and 17, with remanence directions having positive inclinations and a comparable angular separation from the main A cluster, might also be part of A (see Table 2). A third possibility is that the A remanences at sites GU12, 26 and 20 have a significantly different age from those with shallower inclinations. However dykes GU12 and 26 are petrographically identical with dyke GU8, which exhibits the shallow inclination, so independent evidence is lacking that they form a separate generation of dykes. In fact throughout the Taihang swarm, only dyke GU27, with a relative abundance of quartz and myrmekite, has a petrography clearly different from the others and has a palaeomagnetic direction more compatible with a Mesozoic or Cenozoic age.

8 DISCUSSION

8.1 The nature of the characteristic remanence

The positive baked contact tests indicate that the characteristic magnetization in dykes GU12 and 26 is primary in so far that it is not significantly different from that of the baked host rocks and clearly different from that of the unbaked ones. Another indicator of primary remanence is that the chilled margins for dykes GU12, 20, 23 and 26 have the same remanence direction as that in the interiors, but have a significantly higher intensity (Fig. 17), which is to be expected for a chilled margin containing primary magnetite of finer grain size compared with the dyke interior. On this basis, the dyke at site GU23 (representative of the vertical unrotated dykes with shallow remanence inclination) would be construed to have a primary remanence although a baked contact test at the site was inconclusive due to weak and unstable remanence in the host rocks.

We do not know the exact nature of the characteristic A remanence. The positive baked contact test suggests that it is a TRM. However, no host rock samples were collected that clearly showed a hybrid remanence (i.e. the presence of A and the unbaked remanence). These samples not only could have strengthened the positive assessment of the contact tests but might have provided a clue as to whether A in the host rocks was thermal or chemical in nature.

The growth of submicroscopic magnetite in the feldspars that produces the clouding may be a response to slow cooling of the dykes at deeper crustal levels; such grains are known carriers of high-coercivity remanence (Halls & Zhang 1998). If the temperature of the dyke was below the Curie point isotherm for magnetite during the exsolution, a CRM would be produced. If the elapsed time between the initial cooling of the dyke and the growth of magnetite was short compared with the rate of apparent polar wander, the CRM will have a direction indistinguishable from the TRM, and the A remanence will have TCRM characteristics.

This interpretation may explain the local occurrence of A-like remanences in the granulites (Zhang & Piper 1994), which were acquired perhaps chemically at relatively deep crustal levels during or shortly after the Taihang swarm was emplaced.

The unbaked host rocks all have a northerly directed, shallow-inclination component, which is another of the remanence components identified by Zhang & Piper (1994) in their study of NCC granulites, where it appears in about half of their vector plots that decay to the origin (their Figs 9 and 10). The absence of this component within the dykes (Fig. 10) suggests that it is older and therefore should be different between tilted and untilted dykes. However, its direction is not changed significantly by $\sim 20^\circ$ rotations about NW-trending axes. The corresponding virtual pole position (Plat $= \sim 48^\circ$N, Plong $= \sim 278^\circ$E) does not correspond to any part of the Phanerozoic apwp as defined by Enkin *et al.* (1992) and Huang *et al.* (1999), but instead plots in a location, which, given the overall trend of the Proterozoic path, is consistent with a pre-dyke age (see Fig. 19).

One puzzling observation is that the A direction is very similar to that obtained, after structural correction, for Devonian and Silurian strata around the western margin of the NCC (Zhao *et al.* 1993), suggesting that A may be an overprint. On the NCC, Upper Carboniferous limestones and shales directly

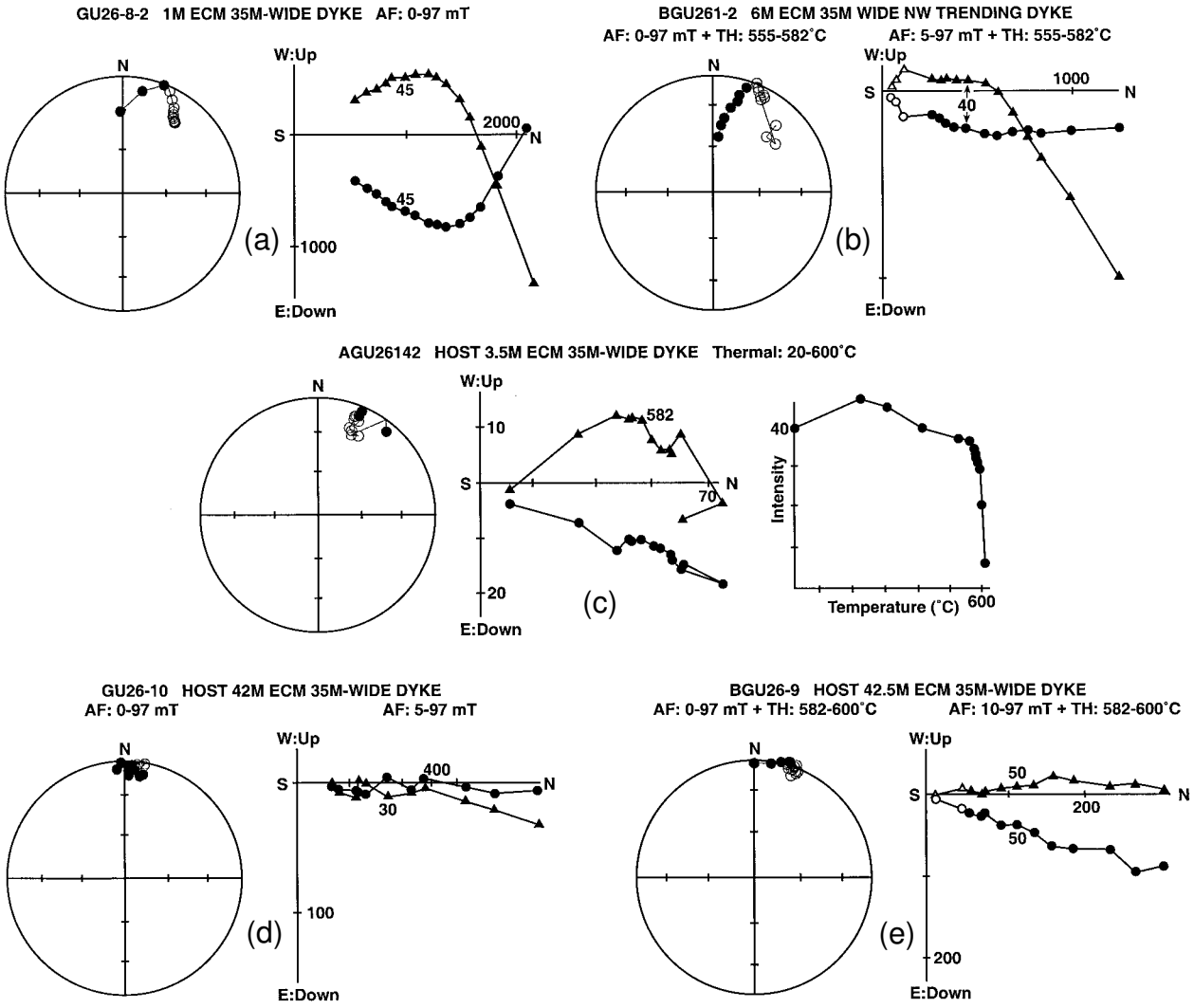

Figure 12. Palaeomagnetic results from site GU26, summarizing the behaviour of the dyke (diagrams a and b), baked tonalitic gneiss (c) and unbaked gneiss (d and e) after AF and thermal demagnetization. In the vector diagrams of (b) and (e), closed/open symbols refer to AF/thermal demagnetization.

overlie Cambro–Ordovician strata conformably, indicating that the craton was a region of non-deposition or erosion during the Silurian and Devonian, and therefore raising the possibility that the NCC was uplifted more or less as a block as a result of Caledonian orogenic activity along both the northern and southern margins of the craton (Lee 1939, p. 108; Hongzhen 1985). The uplift and cooling, together with fluids expelled from the orogens, might thus have led to remagnetization. The A-like remanence in the granulites (Zhang & Piper 1994) and the possible disturbance at 325 Ma $\pm$ 97 Ma shown in the U–Pb plot (Fig. 4) might also support a Middle Palaeozoic overprint scenario. However, two observations lead us to reject the hypothesis: (1) the positive baked contact tests shown by the dykes; and (2) magnetite- and pyrrhotite-bearing Early Palaeozoic strata sampled from three widely spaced locations within the NCC contain no trace of any A-like component (Huang *et al.* 1999). In addition, Huang *et al.* have excluded the Devonian and Silurian data of Zhao *et al.* (1993) from their Palaeozoic apwp, citing incomplete removal of a Permian overprint, and the location of the sampling sites in a terrane that may have rotated relative to the NCC.

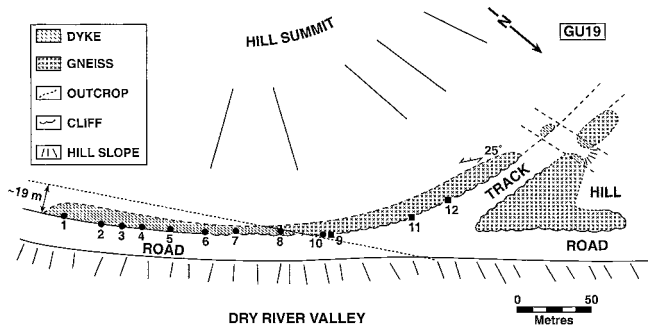

Figure 13. Detailed map of dyke site GU19. Round/square points refer to samples collected by drilling/block sampling.

8.2 Secular variation

The total number of sites used to estimate the direction of remanence A is either 19 or 22. A comparison of palaeomagnetic direction and dyke petrology, attitude and width

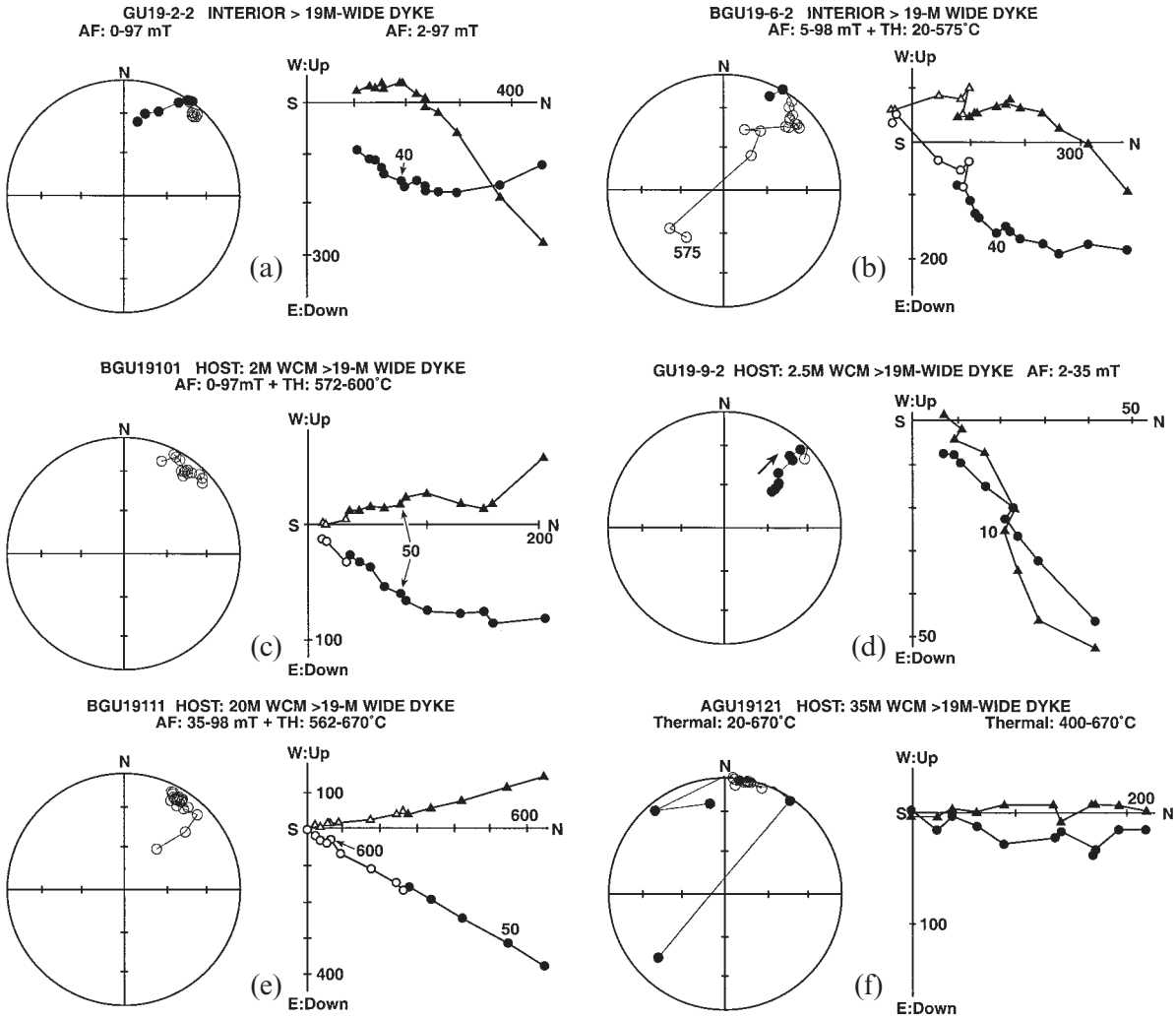

Figure 14. Palaeomagnetic results from site GU19, summarizing the behaviour of the dyke (diagrams a, b) baked gneisses (c, d, e) and possibly unbaked gneiss (f) after AF and thermal demagnetization. Note that all host rock samples appear to be remagnetized by the dyke, except for the most distant one which shows a direction similar to unbaked gneisses at sites GU12 and 26.

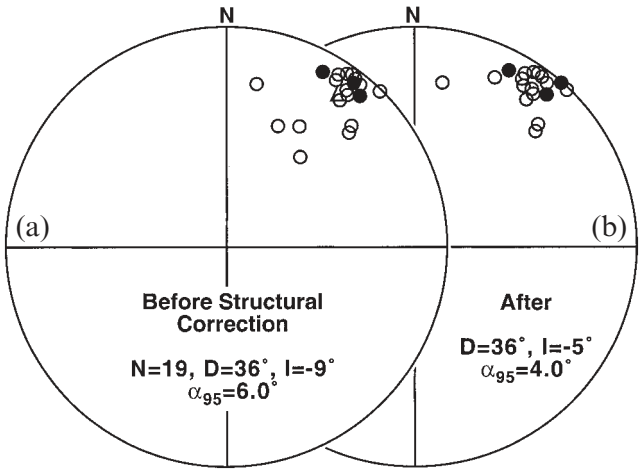

Figure 15. Equal-area stereoplots of site directions from the Taihang dyke swarm (a) before and (b) after structural correction,

between sites gives no obvious correlations except for GU6 and 7, both vertical 35 m wide dykes striking 335° and composed of conspicuously ophitic diabase, and these sites have been combined into one. Where detailed geochemical and palaeomagnetic investigations have been done on a dyke swarm, for example on the 2076 Ma Fort Frances swarm from the Canadian Superior Province (Halls 1986), adjacent dykes are not only palaeomagnetically distinct, but also have small but significant differences in their minor element geochemistry (for example in P_2O_5), indicating that they represent discrete and separate magma pulses, either from separate chambers or from one that had sufficient time to evolve chemically.

For the Taihang dyke swarm, the time span represented by the dykes is unknown. However at site GU21, the eastern side of the dyke exhibits a reversed component which has a higher coercivity and unblocking-temperature spectrum than the normal component with which it coexists (Fig. 18). Across the dyke, the intensities of the higher-coercivity remanence of the normal and reversed components are similar, suggesting their common

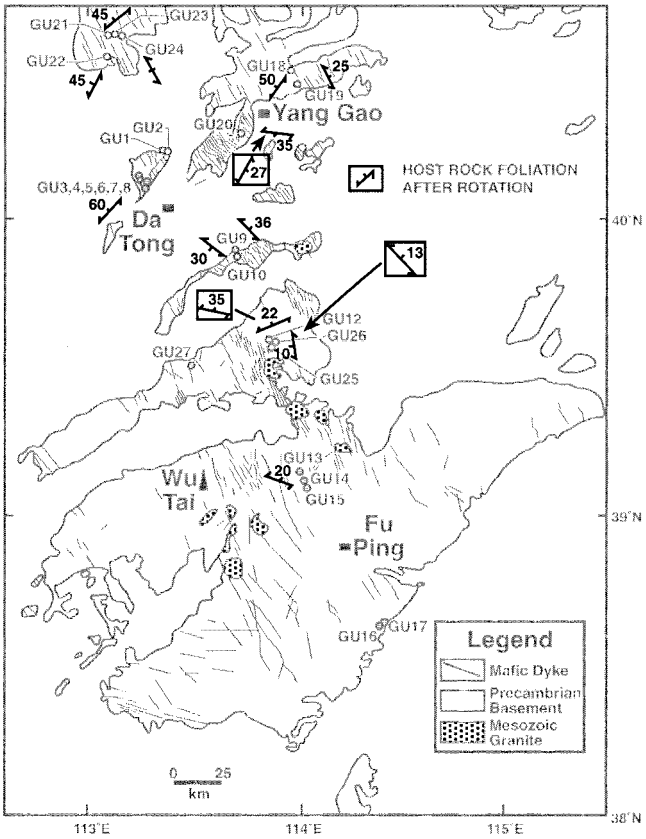

Figure 16. Map showing the observed orientation of gneissic foliation at the dyke sampling localities. Orientations shown in boxes are the values after rotating the dykes at sites GU12, 20 and 26 to the vertical.

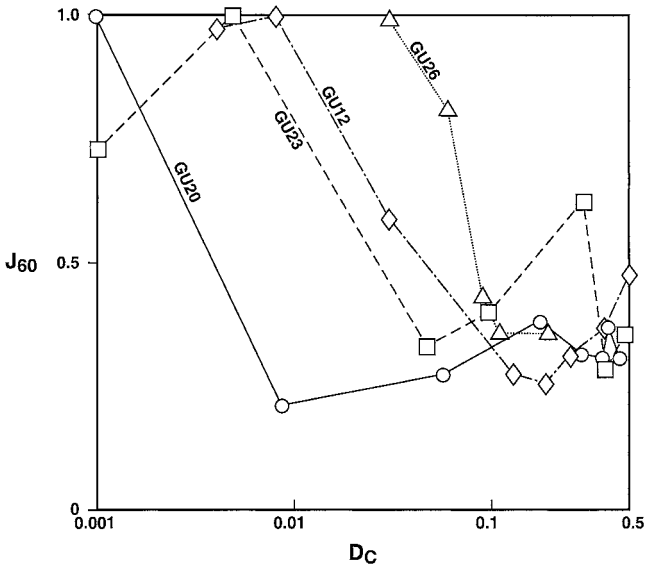

Figure 17. Log-linear plot showing how the intensity of the A component, after AF treatment at 60 mT, varies across four dykes. The value of J_{60}, the magnetization intensity remaining after AF demagnetization at 60 mT, normalized to the maximum value, is plotted against D_C, the distance of the sample from a chilled margin, expressed as a fraction of dyke width. J_{60} was chosen because after 60 mT the remanence is carried only by the A component.

origin. One explanation is that the growth of exsolved magnetite in the cloudy feldspars was in some way delayed, perhaps due to differences in feldspar composition or grain size, and the delay was sufficient to span a magnetic field reversal. This observation might therefore suggest that the remanence residing in cloudy feldspar in different dykes was acquired over a time span sufficient to average out secular variation. The two-tier statistical analysis of Watson & Irving (1957), applied to either the structurally corrected or uncorrected data, gives a between-site circular standard deviation (θ_{63}), freed of the effects of within-site scatter, of about 10°. If the structurally uncorrected data are expanded to include sites 13, 15 and 17, thereby improving the Fisherian distribution, the θ_{63} value increases to 13°. These values are low in comparison with the field over the last five million years, where, for comparable palaeolatitudes (about 3° for the Taihang dykes), a θ_{63} of about 15°–20° would be expected if secular variation was fully included in the data. However a major assumption, the validity of which is unknown, is that the Palaeoproterozoic field was similar in size and behaviour to that of the last 5 Myr. The relatively large number of dykes sampled, the probability that each represents a different magma pulse, and the suggestion of a magnetic field reversal during the time when the characteristic remanence was acquired are taken here as evidence that secular variation has indeed been averaged out.

8.3 Implications for continental reconstructions

The Taihang dyke virtual pole (TD in Fig. 19) plots at the extreme northeastern (~1800 Ma) end of the apwp for the NCC as given by Zhang (1998), and defines the first precisely dated pole for this path. The exact choice of which of the three poles in Table 2 to use for TD is immaterial since they all lie less than 5° from one another.

A major question concerning the NCC is whether or not it was once connected to the Canadian Shield (part of Laurentia) via the Siberian Shield (Siberia). Key poles with ages similar to that of the Taihang swarm are absent from both Siberia and Laurentia (McElhinny *et al.* 1999), although two well-determined poles from Laurentia with significantly different positions have assigned ages that are comparable. The first is from undeformed and unmetamorphosed vertical pegmatite veins which appear to represent the last igneous activity within the Trans-Hudson orogen of the Canadian Shield (Symons *et al.* 2000). Although the veins measured palaeomagnetically are undated, others in their vicinity give monazite or allanite U–Pb ages of 1768 ± 4 Ma (Chiarenzelli 1989). The remanence, considered primary by Symons *et al.* (2000), on the basis of a significantly ($P = 0.05$) different pole position from granites cut by the pegmatite veins, yields a virtual pole at Plat = 67.5°N, Plong = 276°E (dp = 7.6°, dm = 7.8°, $N = 18$ veins). This pole (TH in Fig. 19) plots within a cluster of other poles, all from the Trans-Hudson orogen, that have assigned U–Pb ages from 1849 to 1770 Ma (Symons *et al.* 2000). The second virtual pole (Plat = 15.4°N, Plong = 263.5°E, $A_{95} = 4°$, MD in Fig. 19) comes from a magnetization (the A component of Zhai *et al.* 1994) found in 1.88 Ga Molson dykes that lie adjacent to the Trans-Hudson orogen on its eastern side and which become more deformed by the orogen towards the west. This magnetization, which is an overprint (Halls & Heaman 2000), may

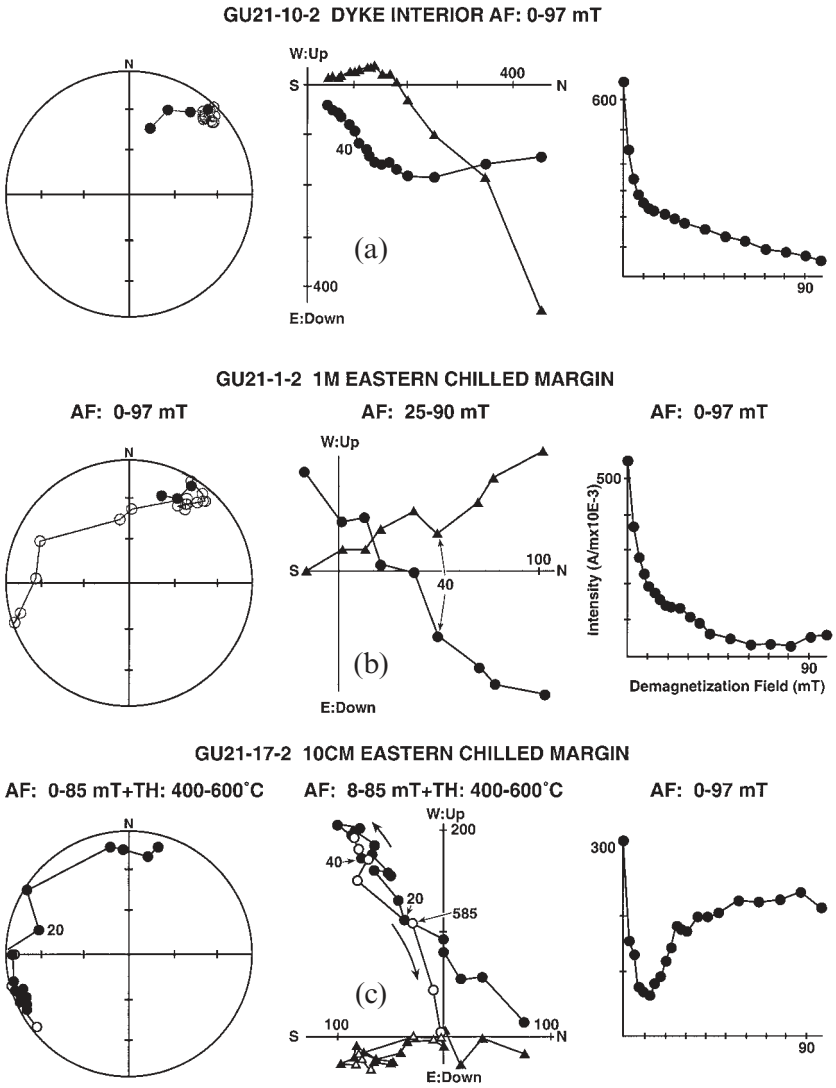

Figure 18. Equal-area stereoplots, vector diagrams and intensity decay plots for three samples from a 31 m wide dyke at site GU21. In (a), the interior sample shows a dominantly single component A magnetization (with a minor low-coercivity PEF component) which is typical of seven other interior samples. In (b), a sample 1 m from the eastern margin shows a weak additional component of higher coercivity and opposite polarity which cannot be isolated due to low magnetization intensity at ~100 mT. In (c), this antipodal component is more strongly developed closer to the chilled margin and is defined by thermal following AF treatment. Solid/open points in the vector diagram are after AF/thermal demagnetization.

be related to the final phase of the orogen, dated by U–Pb on late pegmatites and gneisses in the adjoining Thompson Belt to be from 1720 to 1820 Ma (Machado 1990). This pole also occurs with others of possibly similar age including two which involve mafic igneous rocks: 1827 Ma (U–Pb) Sparrow dykes (McGlynn *et al.* 1974; Bostock & van Breemen 1992) and Kazan flows and dykes (Park *et al.* 1973) that could be older than their provisional ages of ~1720 Ma based on K–Ar and Rb–Sr dates. If the TH, MD and TD virtual poles are rotated to the North geographical pole, the distance between Laurentia and the NCC, presently about 7000 km, can either shrink to about 3500 km if the MD pole is used or increase to about 9500 km if the TH pole is used. These are minimum distances because rotations about the pole are permissible given that palaeolongitude is undetermined. If the MD pole is used, the NCC can move approximately to a position that would be obtained if the Arctic Ocean were closed to join Siberia and Laurentia, and the NCC moves closer to Siberia after removal of the predominantly Phanerozoic crust that forms the intervening Mongolo–Okhotsk orogen (Fig. 20a). If the TH pole is used, the NCC is sufficiently remote from Laurentia that it cannot have been interconnected via Siberia. At the present time we do not know which, if any, of the two poles MD and TH is preferable, because both are associated with the Trans-Hudson orogen and their ages may be more reliably given by Ar–Ar rather than by U–Pb dating methods.

However, tectonostratigraphic comparisons between the NCC, Laurentia and Siberia suggest that these blocks have been together during almost the entire late Palaeoproterozoic to Neoproterozoic interval (Li *et al.* 1996), so that a solution using the MD pole is more inviting. A first-order comparison of the apwp for the NCC and Laurentia (Fig. 19) shows in both cases a wide swath of poles extending from North America to Australasia which on a timescale of ~500 Ma become younger towards the SW, although for periods of the order of ~100 Ma the paths are very different. This observation might suggest that the NCC and Laurentia experienced at least a loose connection with one another during Proterozoic times. A similar

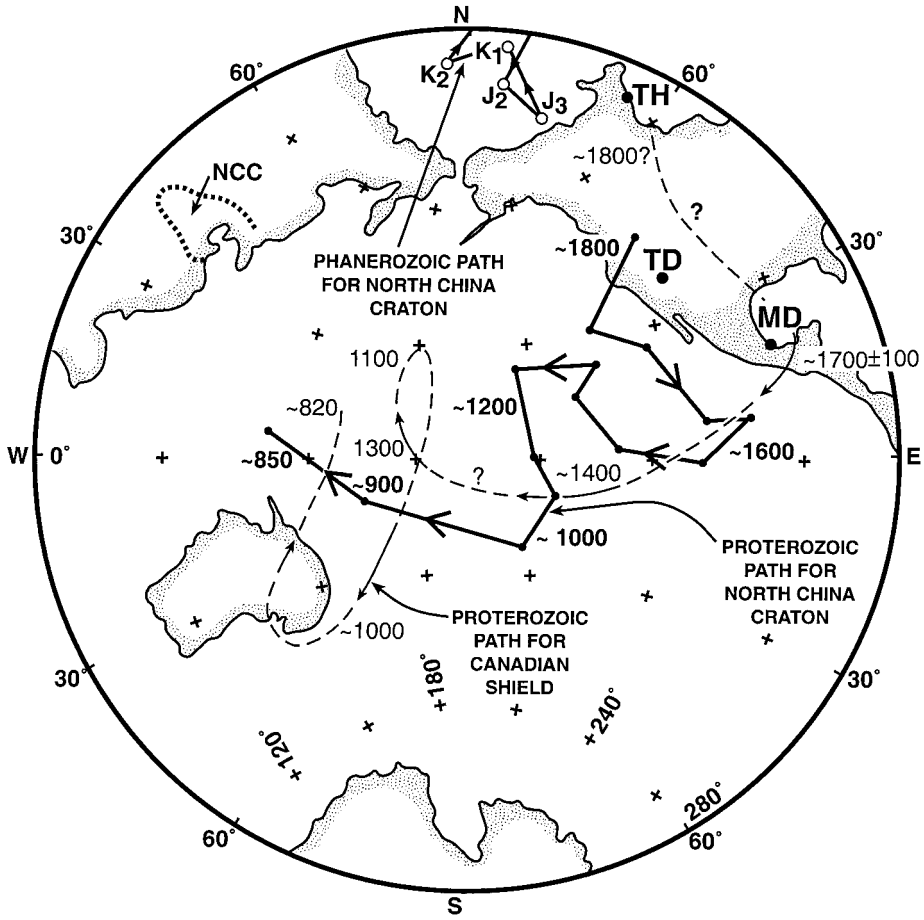

Figure 19. The location of the palaeomagnetic pole for the Taihang dyke swarm (TD) is shown with respect to the Proterozoic apparent polar wander path for the NCC from about 1800 to 800 Ma (after Zhang 1998) for which approximate ages are shown in bold font. The dashed line is a simplified apparent polar wander path for the Canadian Shield part of Laurentia for the same time period, with approximate ages in lighter font, based on data summaries in Symons *et al.* (2000), Kotzer *et al.* (1992) and Costanzo-Alvarez & Dunlop (1998). TH and MD represent two pole positions along this path that may correspond in age to the TD pole. The Jurassic and Cretaceous path for the NCC is from Enkin *et al.* (1992).

'weak union' between Laurentia and Siberia has also been invoked by Smethurst *et al.* (1998) from the Mesoproterozoic (~1.1 Ga) to the end of the Palaeozoic. More specific palaeomagnetic studies (in addition to ours at 1770 Ma) may be cited that allow a close spatial affiliation for the NCC, Laurentia and Siberia, although the data must be treated with caution because they contain no key poles. Data from mafic dykes in the Anabar Massif (Ernst *et al.* 2000) and Vendian red beds in Siberia (Pisarevsky *et al.* 2000) allow a fit of Siberia to Laurentia for the respective time intervals of approximately 1500 Ma and 580–650 Ma more or less in their present-day configurations (Figs 20b and c). Union of the three blocks may extend into the Palaeozoic, although it is demonstrably weaker. For example, Early Palaeozoic (Late Cambrian to Ordovician) poles from the NCC, Siberia and Laurentia (Huang *et al.* 1999; Smethurst *et al.* 1998; Torsvik *et al.* 1996) permit the NCC and Laurentia to occupy positions, relative to one another, that are similar to the present, with Siberia, rotated almost 90° anticlockwise, in between (Fig. 20d). During the Silurian, palaeomagnetic data (see Smethurst *et al.* 1998 for compilation) allow Siberia to remain in the vicinity of the northern margin of Laurentia, and rotated about 30° anticlockwise with respect to the present-day configuration, but the NCC, occupying an equatorial palaeolatitude if the data of Zhao *et al.* (1993) are accepted, cannot be placed on the opposite side of Siberia to Laurentia (Fig. 20e), although it had assumed this position by Middle Jurassic times.

The curious observation is that, despite this evidence for separation, and the existence of intervening fold belts such as the Palaeozoic Innuitian orogen between Laurentia and Siberia, and the Palaeozoic–Mesozoic Mongolo–Okhotsk orogen between Siberia and the NCC, palaeomagnetic data allow the NCC at ~1770 Ma and the Siberian craton at ~1500 Ma and again at ~600 Ma to occupy similar positions and orientations, relative to Laurentia, to those that they currently hold. If the positions at about 1750–1800 Ma of Baltica, Laurentia and the NCC are plotted (Fig. 20f) the position of Baltica relative to Laurentia in terms of orientation and palaeolatitude is similar to that at 1265 Ma (Buchan *et al.* 2000) and little different from that at the present time. According to Torsvik *et al.* (1996), a comparable configuration of Baltica with Laurentia also occurred at 750 Ma (their Fig. 6), and again in the Silurian at 425 Ma (their Fig. 13), despite intervening periods when Baltica assumed other configurations with respect to Laurentia.

A similar coincidence, concerning the Sao Fransisco/Congo craton in South America and the Kalahari craton in Africa is reported by D'Agrella Filho & Pacca (1998). In this study Palaeoproterozic (1.9–2.0 Ga) palaeomagnetic data from the

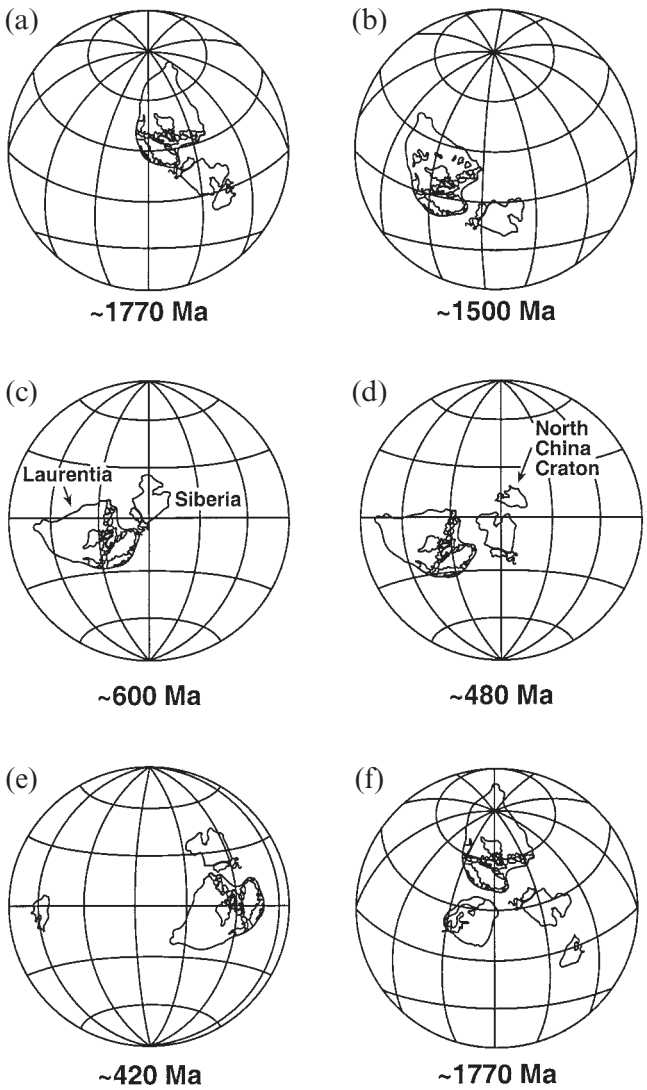

Figure 20. Schmidt projections showing the palaeolatitude and orientation of Laurentia, Siberia, and the NCC at various geological times. (a) At ~1770 Ma Laurentia is positioned using pole MD, the NCC using pole TD, and Siberia, for which there are no relevant palaeomagnetic data, is inserted in between. (b) and (c) Configuration of Siberia and Laurentia at ~1500 Ma (from Ernst *et al*. 2000) and at ~600 Ma (from Pisarevsky *et al*. 2000). (d) Lower Palaeozoic configuration for Laurentia, Siberia and the NCC (~500–470 Ma), based on data from Huang *et al*. (1999), Smethurst *et al*. (1998) and Torsvik *et al*. (1996). (e) Middle Palaeozoic configuration based on data from Smethurst *et al*. (1998), Torsvik *et al*. (1996) and Zhao *et al*. (1993). (f) Configuration including Baltica at ~1770 Ma. Laurentia is positioned using the mean of the two poles MD and TH, and Baltica is according to Elming *et al*. (1993). Each configuration represents only one of many because longitude is unconstrained and the polarity of the Proterozoic magnetic field for each cratonic block is unknown.

two cratons are similar after closure of the Atlantic, implying that intervening Neoproterozoic fold belts do not appear to have led to any displacement between the cratons that is palaeomagnetically detectable. It may therefore be concluded either that there is a propensity for groups of continents to reassemble in preferred configurations despite intervals of wide dispersal, or that they have more or less always remained together, with episodes of relatively modest dispersal that is reversible within the limits of palaeomagnetic detection.

9 CONCLUSIONS

A precisely dated palaeomagnetic pole has been obtained for the 1769 Ma Taihang dyke swarm that cuts the NCC. This pole is considered to be a key anchor pole for the NCC apwp. The pole plots almost exactly on the apwp for the NCC as defined by Zhang (1998) and in the expected time segment. If the pole is compared with those of possible similar age from the Canadian Shield, the NCC can lie in a position and orientation with respect to Laurentia at 1770 Ma which is similar to the present-day configuration. The inference, which must remain cautious in view of the lack of palaeolongitude information and the paucity of key palaeomagnetic poles, is that the NCC, Laurentia, Siberia and Baltica have remained in more or less the same configuration for the last 1770 Ma, despite at least one period of apparent widespread fragmentation and dispersal in the Palaeozoic.

ACKNOWLEDGMENTS

Most samples for this study were collected during fieldtrips in 1996 and 1998. Regarding the first fieldtrip, we (HH, BZ, JL and GH) would like to thank driver Yan Guan for his skill, often displayed under difficult conditions which included road and bridge damage after severe flooding. For the second trip, HH and GH acknowledge the excellent judgement of driver Li Shin Yang in terms of access feasibility, and also thank graduate students Wenyuan He and Liang-shin Ye for providing valuable field assistance. BZ and XQ thank Dr Huangfeng Liu, formerly of the Palaeomagnetic Laboratory, Peking University, for help in the measurement of pilot samples from the Taihang swarm that were obtained in 1986. HH would like to thank Zheng Li, Sergei Pisarevsky and David Evans, all of the Tectonics Special Research Centre, University of Western Australia for helpful discussions, David Symons, Sergei Pisarevsky, Richard Ernst and Ken Buchan for preprints of their papers, Marilyn Fraser for help in sample measurement at the Erindale Palaeomagnetic laboratory, and Alison Dias who drafted the figures. Fig. 20 was drawn with the aid of the GMAP programme of T. Torsvik and M. Smethurst (NGU), the Siberia outline for which was kindly provided by Sergei Pisarevsky. The research was supported by Natural Sciences and Engineering Research Council of Canada grant No. A7824 awarded to HCH, and by a grant from the National Natural Science Foundation of China awarded to JL and XQ. The paper was completed while HCH was a Visiting Research Fellow at the Tectonic Special Research Centre, University of Western Australia.

REFERENCES

Ahrens, L.H., Cherry, R.D. & Erlank, A.J., 1967. Observations on the Th-U relationship in zircons from granitic rocks and from kimberlite, *Geochim. cosmochim. Acta,* **31,** 2379–2387.

Bostock, H.H. & van Breemen, O., 1992. The timing of emplacement, and the distribution of the Sparrow diabase dyke swarm, District of Mackenzie, Northwest Territories, in *Radiometric Age and Isotopic Studies, Rpt. 6, Geol. Surv. Can. Paper 92-2*, pp. 49–55.

Buchan, K.L., Mortensen, J.K. & Card, K.D., 1994. Integrated paleomagnetic and U-Pb geochronologic studies of mafic intrusions in the southern Canadian Shield: implications for the early Proterozoic polar wander path, *Precamb. Res.,* **69,** 1–10.

Buchan, K.L., Mertanen, S., Park, R.G., Pesonen, L.J., Elming, S. & Abrahamsen, N., 2000. Comparing the drift of Laurentia and Baltica in the Proterozoic: the importance of key palaeomagnetic poles, *Tectonophysics,* **319,** 167–198.

Chen, X. & Shi, L., 1994. Mafic dyke swarms associated with extensional tectonics, in *Research on Extensional Tectonics*, pp. 71–74, ed. Qian, X., Geology Publishing House, Beijing (in Chinese).

Chiarenzelli, J.R., 1989. The Nistowiak and Guncoat gneisses: implications for the tectonics of the Glennie and LaRonge domains, northern Saskatchewan, Canada, *PhD* thesis, University of Kansas, Kansas.

Costanzo-Alvarez, V. & Dunlop, D.J., 1998. A regional paleomagnetic study of lithotectonic domains in the Central Gneiss Belt, Grenville Province, Ontario, *Earth planet. Sci. Lett.,* **157,** 89–103.

Davis, D.W., 1982. Optimum linear regression and error estimation applied to U-Pb data, *Can. J. Earth Sci.,* **19,** 2141–2149.

D'Agrella Filho, M.S. & Pacca, I.I.G., 1998. Paleomagnetism of Paleoproterozoic mafic dyke swarm from the Uaua region, north-eastern Sao Fransisco craton, Brazil: tectonic implications, *J. South Am. Earth Sci.,* **11,** 23–33.

Elming, S.-A., Pesonen, L.J., Leino, M.A.H., Khramov, A.N., Mikhailova, N.P., Krasnova, A.F., Mertanen, S., Bylund, G. & Terho, M., 1993. The drift of the Fennoscandian and Ukrainian shields during the Precambrian: a palaeomagnetic analysis, *Tectonophysics,* **223,** 177–198.

Enkin, R.J., Yang, Z., Chen, Y. & Courtillot, V., 1992. Paleomagnetic constraints on the geodynamic history of the major blocks of China from the Permian to the Present, *J. geophys. Res.,* **97,** 13 953–13 989.

Ernst, R.E., Buchan, K.L., Hamilton, M.A., Okrugin, A.V. & Tomshin, M.D., 2000. Integrated paleomagnetism and U-Pb geochronology of mafic dikes of the eastern Anabar Shield region, Siberia: implications for the Mesoproterozoic paleolatitude of Siberia and comparison with Laurentia, *J. Geol.,* **108,** 381–401.

Guo, J. & Shi, X., 1996. Geochronology and important geological events, in *Granulites and Lower Continental Crust in North China Archaean Craton,* pp. 133–149, eds Zhai, M. *et al.,* Seismological Press, Beijing.

Halls, H.C., 1986. Paleomagnetism, structure and longitudinal correlation of Middle Precambrian dykes from northwestern Ontario and Minnesota, *Can. J. Earth Sci.,* **23,** 142–157.

Halls, H.C. & Heaman, L.M., 2000. The paleomagnetic significance of new U-Pb data from the Molson dyke swarm, Cauchon lake area, Manitoba, *Can. J. Earth Sci.,* **37,** 957–966.

Halls, H.C. & Zhang, B., 1998. Uplift structure of the southern Kapuskasing zone from 2.45 Ga dike swarm displacement, *Geology,* **26,** 67–70.

Halls, H.C., Palmer, H.C., Bates, M.P. & Phinney, W.C., 1994. Constraints on the nature of the Kapuskasing structural zone from the study of Proterozoic dyke swarms, *Can. J. Earth Sci.,* **31,** 1182–1196.

Heaman, L.M. & LeCheminant, A.N., 1993. Paragenesis and U-Pb systematics of baddeleyite (ZrO2), *Chem. Geol.,* **110,** 95–126.

Heaman, L.M., Bowins, R. & Crocket, J., 1990. The chemical composition of igneous zircon suites: implications for geochemical tracer studies, *Geochim. cosmochim. Acta,* **54,** 1597–1607.

Hoffman, P.F., 1991. Did the break-out of Laurentia turn Gondwanaland inside-out?, *Science,* **252,** 1409–1412.

Hongzhen, W., compiler, 1985. *Atlas of the Palaeogeography of China,* Cartographic Publishing House, Beijing.

Hou, G. & Mu, Z., 1994. K-Ar ages and geological significance of late Precambrain mafic dyke swarms from the North China Craton, *Shanxi Geol.,* **9,** 267–270 (in Chinese).

Huang, B., Yang, Z., Otofuji, Y. & Zhu, R., 1999. Early Paleozoic paleomagnetic poles from the western part of the North China Block and their implications, *Tectonophysics,* **308,** 377–402.

Kirschvink, J.L., 1980. The least squares line and plane and the analysis of paleomagnetic data, *Geophys. J. R. astr. Soc.,* **62,** 699–718.

Kotzer, T.G., Kyser, T.K. & Irving, E., 1992. Paleomagnetism and the evolution of fluids in the Proterozoic Athabasca basin, northern Saskatchewan, Canada, *Can. J. Earth Sci.,* **29,** 1474–1491.

Krogh, T.E., 1973. A low contamination method for hydrothermal decomposition of zircon and extraction of U and Pb for isotopic age determinations, *Geochim. cosmochim. Acta,* **37,** 485–494.

Krogh, T.E., 1982. Improved accuracy of U-Pb ages by the creation of more concordant systems using an air abrasion technique, *Geochim. cosmochim. Acta,* **46,** 637–649.

Lee, J.S., 1939. *The Geology of China,* Thomas Murby Publishers, London.

Li, J., 1999. Tectonic constraints from Chinese cratonic blocks for reconstruction of Rodinia, in *European Un. Geoscientists Mtg, J. Conf. Abstracts,* **4,** 21–22.

Li, J. & Qian, X., 1994. *The Early Precambrian Crustal Evolution of Hengshan Metamorphic Terrain, North China Craton,* Shanxi Science and Technology Press, Taiyuan (in Chinese).

Li, H., Li, H. & Lu, S., 1995. Single grain zircon U-Pb ages for volcanic rocks from Tuanshanzi Formation of Changcheng system and their geological implications, *Geochimica,* **24,** 43–48 (in Chinese).

Li, J., Qian, X., Zhai, M. & Guo, J., 1996a. Tectonic division of high-grade metamorphic terrains and late Archean tectonic evolution in north-central part of North China craton, *Acta Petrol. Sinica,* **12,** 179–192 (in Chinese).

Li, Z.X., Zhang, L., Powell, C. & McA., 1996b. Positions of the East Asian cratons in the Neoproterozoic supercontinent Rodinia, *Austral. J. Earth Sci.,* **43,** 593–604.

Li, J., Qian, X. & Zhai, M., 1997. The tectonic division of north China granulite facies belt and its early Precambrian tectonic evolution, *Sci. Geol. Sinica,* **32,** 254–266 (in Chinese).

McElhinny, M.W., Lock, J. & Smethurst, M., 1999. IAGA Global Paleomagnetic Database, http://dragon.ngu.no.

Machado, N., 1990. Timing of collisional events in the Trans Hudson orogen, in *The Early Proterozoic Trans-Hudson Orogen of North America,* pp. 433–441, eds Lewry, J.F. & Stauffer, M., *Geol. Assoc. Canada, Special Paper 37*.

McGlynn, J.C., Hanson, G.N., Irving, E. & Park, J.K., 1974. Paleomagnetism and age of Nonacho Group Sandstones and associated Sparrow Dikes, District of Mackenzie, *Can. J. Earth Sci.,* **11,** 30–42.

Moores, E.M., 1991. Southwest U.S.–East Antarctic (SWEAT) connection: a hypothesis, *Geology,* **19,** 425–428.

Park, J.K., Irving, E. & Donaldson, J.A., 1973. Paleomagnetism of the Precambrian Dubawnt Group, *Bull. geol. Soc. Am.,* **84,** 859–870.

Pisarevsky, S.A., Komissarova, R.A. & Khramov, A.N., 2000. New palaeomagnetic result from Vendian red sediments in Cisbaikalia and the problem of the relationship of Siberia and Laurentia in the Vendian, *Geophys. J. Int.,* **140,** 598–610.

Qian, X. & Chen, Y., 1987. Late Precambrian mafic swarms of the north China craton, in *Mafic Dyke Swarms*, pp. 385–391, eds Halls, H.C. & Fahrig, W.F., *Geol. Assoc. Canada, Special Paper 34.*

Smethurst, M.A., Khramov, A.N. & Torsvik, T.H., 1998. The Neoproterozoic and Paleozoic paleomagnetic data for the Siberian Platform: from Rondinia to Pangea, *Earth Sci. Rev.,* **43,** 1–24.

Sun, D., Li, H., Lin, Y., Zhan, H., Zhao, F. & Tang, M., 1991. Precambrian geochronology and chronotectonic framework and model of chronocrustal structure of the Zhongtiao Mountains, *Acta Geol. Sinica,* **65,** 216–231 (in Chinese).

Symons, D.T.A., Symons, T.B. & Lewchuk, M.T., 2000. Paleomagnetism of the Deschambault pegmatites: stillstand and hairpin at the end of the Paleoproterozoic Trans-Hudson Orogeny, Canada, *Phys. Chem. Earth,* **25,** 479–487.

Torsvik, T.H., Smethurst, M.A., Meert, J.G., Van der Voo, R., McKerrow, W.S., Brasier, M.D., Sturt, B.A. & Walderhaug, H.J., 1996. Continental break-up and collision in the Neoproterozoic and Paleozoic—A tale of Baltica and Laurentia, *Earth Sci. Rev.,* **40,** 229–258.

Van der Voo, R., 1988. Palaeozoic palaeogeography of North America, Gondwana and intervening displaced terranes: comparisons of palaeomagnetism with palaeoclimatology and biogeographical patterns, *Geol. Soc. Am. Bull.,* **100,** 311–324.

Watson, G.S. & Irving, E., 1957. Statistical methods in rock magnetism, *Mon. Not. R. astr. Soc., Geophys. Suppl.,* **7,** 289–300.

Wilde, S., Cawood, P. & Wang, K., 1997. The relationship and timing of granitoid evolution with respect to felsic volcanism in the Wutai complex, North China Craton, in *Precambrian Geology and Metamorphic Petrology*, pp. 75–87, eds Qian, X., You, Z. & Halls, H.C, *Proc. 30th Int. Geol. Cong.,* VSP, Utrecht, the Netherlands.

Yan, Y., Li, J. & Liu, W., 1996. Huaian Massif and Hengshan Massif, in *Granulites and Lower Continental Crust in North China Archaean Craton,* pp. 55–131, eds Zhai, M. *et al.,* Seismological Press, Beijing.

Zhai, M., Li, Y. & Guan, H., 1996. Archaean granites and cratonization, in *Granulites and Lower Continental Crust in North China Archaean Craton,* pp. 151–188, eds Zhai, M. *et al.,* Seismological Press, Beijing.

Zhai, Y., Halls, H.C. & Bates, M.P., 1994. Multiple episodes of dike emplacement along the northwestern margin of the Superior Province, Manitoba, *J. geophys. Res.,* **99,** 21 717–21 732.

Zhang, B., 1988. Prelimary research on Late Precambrian mafic dyke swarms in Luliang-northern Shanxi: their Paleomagnetism, *MSc thesis,* Peking University, Beijing (in Chinese with English abstract).

Zhang, H., 1998. Preliminary Proterozoic apparent polar wander paths for the South China block and their tectonic implications, *Can. J. Earth Sci.,* **35,** 302–320.

Zhang, J. & Piper, J.D.A., 1994. Magnetic fabric and post-orogenic uplift and cooling magnetizations in a Precambrian granulite terrain: The Datong-Huai'an region of the North China Shield, *Tectonophysics,* **234,** 227–246.

Zhao, X., Coe, R.S., Wu, H. & Zhao, Z., 1993. Silurian and Devonian paleomagnetic poles from North China and implications for Gondwana, *Earth planet. Sci. Lett.,* **117,** 497–506.

Zhao, T., Guan, B. & Tu, S., 1994. Some problems with the study of the volcanic rocks of the Xionger Group on the southern margin of the North China plate, *Geol. Rev.,* **40,** 446–455 (in Chinese).